의학박사 학위논문

Studies on Enzymatic Activity and Protein Stability of Rab6A′ and Rab11A by crystal structure

단백질 결정구조를 통한 Rab6A’과 Rab11A의 효소적 활성 및 단백질 안정성에 대한 연구

2016년 08월

서울대학교 대학원

의과학과 의과학 전공

신 영 철

A thesis of the Degree of Doctor of Philosophy

단백질 결정구조를 통한 Rab6A’과 Rab11A 의 효소적 활성 및 단백질 안정성에 대한 연구

Studies on Enzymatic Activity and Protein Stability of Rab6A′ and Rab11A by crystal structure

August 2016

The Department of Biomedical Sciences,
Seoul National University
College of Medicine
Young-Cheul Shin

Studies on Enzymatic Activity and Protein Stability of Rab6A′ and Rab11A by crystal structure

by
Young-Cheul Shin

A thesis submitted to the Department of Biomedical Sciences in partial fulfillment of the requirements for the Degree of Doctor of Philosophy in Biomedical Science at Seoul National University College of Medicine

August 2016

Approved by Thesis Committee:

Professor _____Chairman
Professor _____Vice chairman
Professor _____
Professor _____
Professor _____

ABSTRACT

The Ras-superfamily of small GTP-binding proteins (GTPase), plays critical roles in various cellular processes. The activity of this family is controlled by the states of nucleotide binding. When GTP binds to GTPase, it becomes the active form. Once GTP is hydrolyzed to GDP + Pi, the GTPase becomes the inactive form. Rab GTPase is Ras-superfamily and plays an especially important role in vesicle trafficking, which is essential for endocytosis, biosynthesis, secretion, cell differentiation and growth. Because a functional loss of the Rab pathways has been implicated in a variety of disease, the Rab GTPase family has been extensively investigated. Mutant form of Rab GTPase has been commonly utilized for biochemical study of Rab and Rab-related functional studies. Generally, most mutants in catalytic region of Rab GTPase have been constructed by sequence alignment from other GTPases which are already known as active- or inactive form by structural study or biochemical study. Since similar structural of GTPases could show different functional profile, such as binding affinity of ligand, rate of enzyme activity and interacting partners, it is possible that mutation of similar position of amino acid likely

showed different activity between Rab GTPases. Therefore, functional activity and molecular mechanism of Rab GTPase mutants must be validated by biochemical analysis and structural analysis. Due to this reason, I undertook to characterize the activity of Rab GTPase mutants. In this study, I crystallized mutant form of Rab6A′ and Rab11A and solved crystal structures of them.

In the first part, I solved crystal structure of active form of Rab6A and I found that active form of GTPase could trap GDP. This observation indicated that binding of ligand could be various dependent on protein-type and environment around protein. In second part, I found that the stability of inactive Rab11A depended on the occupation of GDP. In the third part, active Rab11A could trap GTP instead of hydrolyzing it, because of absence of water molecule around catalytic pocket. These results provide evidence of functionally association of Rab6A and Rab11A and better understanding for Rab-related network and diseases.

Keywords: Small G protein, Ras superfamily, Rab GTPase, Rab6A, Rab11A, Membrane trafficking, Crystal structure

Student number: 2009-21890

CONTENTS

LIST OF TABLES AND FIGURES

Chapter 1

Chapter 2

Chapter 3

LIST OF ABBREVIATION

FPLC : fast performance liquid chromatography

His-tag : six repeated polyhistidine-tag

PEG : polyethylene glycol

SDS : sodium dodecyl sulfate

SDS-PAGE : SDS polyacrylamide gel electrophoresis

Ni-NTA : Nickel-nitrilotriacetic acid resin

E1 on SDS-gel data : #1 eluted fraction

INTRODUCTION

The Ras-superfamily of small G proteins is a family of GTP hydrolases that comprises more than 150 members in eukaryotes from yeast to human [1, 2]. The activity of this family is regulated by the GTP binding state: GDP-bound inactive and GTP-bound active forms[3]. Most of them are ubiquitously present inside cells and this superfamily is structurally classified into five principal families (Ras, Rho, Rab, Arf, and Ran) which are involved in a wide variety of cellular processes including proliferation, differentiation, cell adhesion, metabolism, contraction, motility, survival, and apoptosis [4]. The common structures of GTPases are central six-stranded β sheet flanked by five α helices on both sides. Each GTPase has conserved amino acid sequences of the enzymatic active site that are responsible for specific interactions with GDP and GTP molecules [5]. The activity of GTPase is mainly regulated by bound guanine nucleotides, with the GTP- and GDP bound form indicating the active and inactive state, respectively [3, 6, 7]. These forms are interconvertible via GDP/GTP exchange and GTPase reactions, and the transition between the active and inactive form is accompanied by the conformational changes in

two highly mobile regions, the switch I and switch II domains [8]. To transit to the active state, GTPase needs to bind the GTP and Mg^{2+} ion in switch I and the phosphate-binding loop (P-loop) domain, which lasts until the GTP is hydrolyzed by the switch II domain [8]. GTP/Mg^{2+}binds more strongly to GTPase than GDP/Mg^{2+} [9]. After hydrolysis of the GTP to GDP and Pi, the GDP-bound inactive state of the GTPase releases the Mg^{2+} when the GTPase opens its switch I domain, leading to the release of the GDP [8, 10]. This allows binding of GTP to the GTPase and return to the active state, thereby completing the mechanism. This mechanism is cyclical in physiological nature and therefore is called the GTPase cycle [10, 11]. During the GTPase cycle, the GTPase transduces the upstream signal to the downstream effectors via regulators related to the binding, hydrolysis and release of nucleotides such as GEFs, GAPs and GDIs [11].

The Rab GTPase family is one of the Ras-superfamily of small G proteins. Most of this family of proteins are ubiquitously present inside cells and are key components to various cellular processes, including cytoskeletal organization, mitogenesis, vesicle trafficking, and nuclear transport [12]. Rab family

cycles extensively between the cytoplasmic surface of intracellular membranes and the cytosol regulated by bound state of guanine [13]. Once the newly translated Rab GTPase with inactive state, GDP-bound form first associates with a Rab escort protein (REP), which directs it to Rab geranylgeranyl transferase (RabGGT) [14, 15]. RabGGT consists of α and β subunits which allow Rab GTPase to receive dual prenylation (geranylgeranylation) tails in its C-terminus [16, 17]. After transferase reaction, GTPase is inserted into donor membrane. During this process Rab GTPase can retain in cytosol, if the Rab-REP-RabGGT did not form a complex [17]. After insertion of complex to donor membrane, REP dissociates from the Rab GTPase. The membrane-inserted Rab GTPase is activated by a guanine nucleotide exchange factor (GEF) which converts Rab GTPase to a GTP-bound active form by replacement of GDP to GTP. The active form of the Rab GTPase then recruits specific binding partners, such as sorting adaptors, tethering factors, and motor proteins, and is involved in vesicle formation, transport, and tethering [13, 18-25]. The active form of GTP-bound Rab GTPase becomes inactivated by GTPase activating proteins (GAPs) which accelerate intrinsic

rate of GTPase activity [15, 26, 27]. Then inactivated GTPase is recycled back to cytosol and binds GDP dissociation inhibitor (GDI) [13]. The reinsertion of Rab GTPase to membrane is assisted by a GDI dissociation factor (GDF) and Rab GTPase begins the cycle again [28, 29].

Intracellular membrane traffic is a complex network that connects various organelles of cells, and Rab GTPases are recognized as master regulators by interacting with their myriad effectors localized in specific compartment. Rab1 localizes ER and Golgi, and it regulates ER to Golgi traffic [15, 30, 31]. While Rab2 localizes ER, Golgi and ER–Golgi intermediate compartment (ERGIC) and involves in retrograde traffic, or recycling, from Golgi and the ERGIC back to the ER [32]. Rab6 localize Golgi and it involves in the trans–Golgi network (TGN), as well as exocytic traffic to the plasma membrane [15, 30, 31, 33]. Rab8 localize cell membrane, vesicles and primary cilia [34], Rab10 localize Golgi, basolateral sorting endosomes, GLUT4 (Glucose transporter type 4) vesicles [35, 36], and Rab14 localizes Golgi, early endosome (EE) and GLUT4 vesicles [37, 38]. Despite different cellular localizations between Rab members, they involves in

biosynthetic traffic from the trans-Golgi network (TGN) [39-43]. The GLUT4 associates to Rab GTPases in GLUT4 vesicle and uses them to arrive at the plasma membrane. Several secretory vesicles use Rab3 and granules use Rab26, Rab27 and Rab37 to exocytose their cargo [40, 44-47]. Rab27 involves in melanosome transport that uses Rab32 and Rab38 for TGN to melanosome [48-50]. There are many of Rab GTPases for endosome trafficking, and the major localization is the EE. Rab5 is major regulator in early endocytic steps, which involved in early endosome fusion [32, 51-53]. Lysosome uses Rab7 for degradation or recycling compartments backs to the plasma membrane [32, 54]. Rab15 involves membrane traffic from the early endosome to the recycling endosome [42, 55]. Rab4 regulates fast endocytic recycling while Rab11 regulates slow endocytic recycling [56-58]. Targeting of lipid droplets to organelles is mediated by Rab18. Rab18 localizes Golgi and lipid droplets and it regulates organelles interaction between lipid droplet and ER [17, 59]. Rab24 and Rab33 localize ER and Golgi respectively, and they mediate autophagosome formation [42, 60-62]. Rab45 is reported that induces apoptosis through activation of caspases [63]. Rab21 and Rab25 associate with

subunits of integrin as effector proteins to control cell adhesion and cytokinesis [64–67]. Rab13 localizes tight junctions and regulates their formation in polarized epithelial cells [68]. Rab17 localizes recycling endosomes and regulates transcytosis [69, 70]. Rab19, Rab30, Rab36, Rab39 and Rab41 are found in Golgi, but membrane traffic pathway and function of them are unclear [71–75]. In addition, some of Rab members are poorly characterized, such as Rab28, Rab42 and Rab44.

Since the membrane traffic plays a significant role in cellular process, Rab GTPase is involved in various diseases. Unlike Ras, Ral and Rho GTPases, the role of Rab GTPases in oncogenesis is less well-known. However, several Rab GTPase showed aberrant expression in various types of cancers [76]. Rab1 is upregulated in tongue squamous cell carcinoma, Rab2 in peripheral blood mononuclear cells from solid tumors, Rab3 in nervous system cancers, Rab5 in lung cell adenocarcinoma, Rab20 in exocrine pancreatic carcinoma, and high levels of Rab31 mRNA are associated with breast cancers [77–81]. Among Rab members, Rab25 is well characterized in cancers. It has been reported that Rab25 associated with ovarian and breast cancers including testicular tumor, nephroblastomas,

bladder and hepatocellular carcinomas [82–85]. Interestingly, however, the role of Rab25 differs from cancer subtypes, because reduced expression of Rab25 is found in colorectal adenocarcinomas and colon tumors [86, 87]. In addition, several Rab GTPases associates with anticancer drug. P-glycoprotein is a large transmembrane protein which is overexpressed in multidrug resistance cancer cells. It localized at the plasma membrane extruding anticancer drug and thus decreases drug accumulation inside cell [88]. In drug resistance cells, overexpressed Rab4 decreases surface expression levels of P-glycoprotein, leading to increasing drug sensitivity [89]. Rab6 are also associates with drug accumulation although exact mechanism and phenotype has been unclear [90]. Since Rab GTPases are implicated in various diseases and involved in resistance to anticancer drugs, thus they might be attractive target for anti-cancer therapy.

Rab GTPases are also implicated in several neurological diseases, such as Parkinson's disease (Rab1), Carpenter syndrome (Rab23), Charcot-Marie-Tooth Disease (Rab7), and Alzheimer's disease (Rab5, Rab6 and Rab11) [15, 91–95]. Rab11 is a well characterized member in neurological diseases.

It is involved in the control of TfR recycling and its routing to the exit from recycling endosomes [96, 97]. The functions of the Rab11 family have also been found in various places in the cell, including mobilization of endosomal membranes for phagocytosis in macrophages [98]. Rab11 has been implicated in various diseases including Alzheimer's disease, Huntington disease and Type 2 diabetes [95]. In Alzheimer's disease, pathogenesis is triggered by the accumulation of the β-amyloid which is generated by β and γ secretases. It has been reported that transport of β-amyloid uses Rab11-positive recycling vesicles and Rab11 mediates recycling of β-secretase to the plasma membrane [95]. Other Rab member that involves in Alzheimer's disease is Rab6. Although there is no well-documented relationship between Rab6 and diseases, several study reported that Rab6 is involved in modulation of unfolded protein response (UPR) which is activated in Alzheimer's Disease [92]. In addition, increased level of Rab6 was observed in brains from patients with Alzheimer's Disease [99]. These studies show indirect relationship between Rab11 and Rab6 in Alzheimer's Disease. Furthermore, supporting evidences that functional association with Rab11 and Rab6 in Alzheimer's

Disease are reported. β2-Adrenergic Receptor (β2AR), which is Gs coupled receptor, is involved in production of β-amyloid via stimulation of γ secretase [100, 101]. β2AR specifically interact with Rab11 and Rab6, and it modulates geranylgeranylation by forming complex with RabGGT [25]. Moreover, functional associations between Rab11A and Rab6A are also observed in infected disease and X-linked recessive disorder. In Chlamydia trachomatis, Chlamydia subverts Golgi structure and Rab11A and Rab6A are key regulators in this pathway [102]. In normal cell, golgin-84 regulates Golgi stability. However, inhibition of golgin-84 in infected cell allows Rab11A and Rab6A to recruit chlamydial inclusions [86]. This leads fragmentation of the Golgi apparatus that enhances the number of infectious bacteria in development of Chlamydia trachomatis [103]. In Lowe syndrome, the mutation on rab-binding domain of OCRL (Oculocerebrorenal syndrome of Lowe) protein causes disease and this weakens binding of Rab6A to OCRL [104]. While, Rab11A does not interact with OCRL, it regulates membrane trafficking of TRPV6 which shows elevated expression on surface membrane of OCRL mutant cell [105, 106]. Increased Ca^{2+} absorption by TRPV6 is suppressed

by normal OCRL but not by Disease-caused mutant of OCRL [106]. In addition to functional association between Rab11A and Rab6A in disease, Rab11A and Rab6 are coordinated in mitosis and cytokinesis. Rab11A interacts with FIP3 and they involved in the delivery of endocytic vesicles for cell abscission at the apex of the cleavage furrow [107]. Rab6 interacts with Rabkinesin-6/MKlp2 (Rab6A) and GAPCenA/p150^{Glued} (Rab6A′). These participate in signaling pathways of the metaphase/anaphase transition [108]. In addition, active form of Rab11A and Rab6A share partner protein observed in interphase cells. Rab6-interacting protein 1 (R6IP1), which is identified as a Rab6 partner, also binds to Rab11A [19].

Structural and mutagenesis studies of Rab11A and Rab6A provide better understanding of function of Rab-related traffic network and suggest the possibility of therapeutic approaches for above-described diseases. In addition, structural study of specific transition state of Rab11A and Rab6A is needed for understanding of functional specificity and unique property between Rab GTPases. Furthermore, domain rearrangement dependent of substrate is critical to understanding of effector protein docking because it is well known that effectors

recognize Switch domain determinants that distinguish partner from another protein. Despite, however, the functions of active- and inactive form of Rab11A and Rab6A′ are well studied, structure of them were not resolved. Although structures of Rab11A and its binding partners are resolved, most of them use GTP-analogues for maintaining active form. Interestingly, Rab11A Q72L was used as an active form but natural GTP was hydrolyzed to GDP in the structure. Previously, it is reported that the GTPase activity of Rab11A Q70L was stimulated by GAP effector protein [64], while Rab11A S20V displayed specific binding of GTP and did not exhibit intrinsic and GAP-stimulated GTPase activity, indicating that Rab11A S20V, not Q70L, acts as a dominant GTPase-deficient mutant [109]. However, it was still unclear how Rab11A S20V could be active form.

In this point, I solved crystal structures of Rab6A′ and active form of Rab11A. In first chapter, I report the crystal structure of the mutant form of human Rab6A′ (Q72L), which has been shown to be in a GTP lock form, at 1.9 Å resolution to better understand the functional uniqueness of Rab6A′ and determine the molecular mechanism by which GTP and GDP

control activity. Despite of low intrinsic activity, crystal structure of Rab6A′ was solved GDP bound form. This result is thought that glutamine on P-loop activate water molecule which involved in GTP hydrolysis. In addition, switch I lost its stability which is commonly observed in GDP bound form. In second chapter, I solved and analyze structure of Rab11A. In this study, I report the crystal structure of the constitutively active mutant form of human Rab11A S20V, which has been shown to be in a GTP-locked form, at a resolution of 2.4 Å to better understand the functional uniqueness of Rab11A and determine the molecular mechanism by which GTP and GDP control activity. The structure generated herein showed that Rab11A exists as monomer in solution. Interestingly, there was an endogenous GTP in the nucleotide binding pocket in Rab11A, indicating that Rab11A S20V is a non-hydrolyzable GTPase that accommodates GTP and can contain endogenous GTP without adding nucleotides during the purification step. Although small structural differences were detected at the switch I region, the overall structure of Rab11A S20V with GTP complex is similar to that of other nucleotide-bound Rab11A, possessing Mg^{2+} in the nucleotide binding pocket. Interestingly,

I found that substitution of V20 of Rab11A interferes with proper localization of functionally important water molecules, resulting in GTP being locked in an active form of Rab11A S20V. I also did further study for finding the structural connection of Rab6A and Rab11A. PIST is Golgin family which associates with Golgi membrane and is known as Rab6A binding protein without alter its GTP activity [110]. I crystallized PIST, but failed to determine its structure due to the absence of similar structure for molecular replacement [111]. I also did complex study of Rab11A and TRPV6, which is known as binding partner. Unfortunately, I purified GDP-bound inactive mutant (S25N) of Rab11A and found that Rab11A S25N mutant had an extremely low stability compared with wild type and other mutants. Further analysis revealed that Rab11A S25N has low affinity for GDP, and that the stability of Rab11A S25N depends on the existence of GDP in the nucleotide binding pocket of the protein. I successfully increased the stability and purified Rab11A S25N by a treatment consisting of extra GDP during purification steps and I reported this result in third chapter. These finding open up the opportunity for gaining more insights into the role in Rab-related network and diseases.

CHAPTER 1

Crystal structure of Rab6A'(Q72L) mutant reveals unexpected GDP/Mg^{2+} binding with opened GTP-binding domain

MATERIALS AND METHODS

1. Protein expression and purification

The methods used for expression and purification methods in this study have been described elsewhere in detail. Briefly, human Rab6A′ (Q72L), which corresponds to amino acid residues 5–178, was expressed in BL21 (RIPL) Escherichia coli competent cells under overnight induction at 293 K. Rab6A′ (Q72L) contained a N−terminal His−tag and was purified by nickel affinity chromatography followed by gel−filtration chromatography over a Superdex 200 gel−filtration column (GE Healthcare) that had been pre−equilibrated with a solution of 20 mM Tris pH 8.0 and 150 mM NaCl. The target protein was concentrated to 10–12 mg ml−1.

2. Crystallization and data collection

The crystallization conditions were initially screened at 293 K by the hanging−drop vapor−diffusion method using various screening kits. Initial crystals were grown on plates by equilibrating a mixture containing 1 μl protein solution (4.53 mg ml−1 protein in 20 mM Tris pH 8.0, 150 mM NaCl) and 1 μl of

reservoir solution containing 18% PEG 8000, 0.2 M calcium acetate and 0.1 M sodium cacodylate pH 6.5 against 0.4 ml of a reservoir solution. Crystals appeared within 3 days and grew to maximum dimensions of 0.2 × 0.2 × 0.1 mm in the presence of 20% PEG 8000, 0.3 M calcium acetate and 0.1 M sodium cacodylate pH 6.7. A 1.9 Å native diffraction data set was collected from a single crystal at the beamline BL-4A at the Pohang Accelerator Laboratory (PAL), South Korea. The data sets were indexed and processed using HKL2000 [112].

3. Structure determination and analysis

The structure was determined by molecular replacement phasing method using Phaser. The previously solved structure of GTP-bound Rab6A (PDB code: 2GIL) [113] was used as a search model. Model building and refinement were performed by COOT [114] and Refmac5 [115], respectively. Water molecules were added using the ARP/wARP function in Refmac5. The final model contained residues 13-174 for the A chain and residues 12-175 for the B chain. One GDP/Mg^{2+} was placed at each chain. The geometry was inspected using PROCHECK and was found to be reasonable. A total of 93.98%

of the amino acids were located in the most favorable region and 6.02% were in the allowed regions of the Ramachandran plot. The data collection and refinement statistics are summarized in Table 1. All the molecular figures were generated using the program Pymol (The pymol Molecular Graphics System (2002), DeLano Scientific, San Carlos, USA).

4. Protein Data Bank accession code

The coordinate and structure factor have been deposited in the Protein Data Bank (PDB) with Accession code 4DKX.

Data collection	Native
X-ray source	BL-4A, PAL
Wavelength (Å)	0.9999
Space group	$P22_12_1$
Cell dimensions	
a, *b*, *c*	36.84 Å, 96.78 Å, 109.99 Å
Resolution	50-1.9 Å
R_{sym}[a]	8.9% (48.7%)
Mean $I/\sigma(I)$[a]	29.1 (3.6)
Completeness[a]	99.8% (99.9%)
Redundancy[a]	6.7 (6.7)
Refinement	
Resolution	50-1.9 Å
No. of reflections used	30283
R_{work}/R_{free}	19.6%/25.0%
No. of atoms	
Protein	2484
Water and other small molecule	305
Average *B*-factors	25.0 $Å^2$
R.m.s deviations	
Bond lengths	0.028 Å
Bond angles	3.175°
Ramachandran plot	
Most favored regions	93.98%
Additional allowed regions	6.02%

a Highest resolution shell is shown in parenthesis

Table 1. Crystallographic statistics.

RESULTS

Crystallization of Rab6A′ (Q72L)

Three different types of Rab6 has been identified in mammals (Rab6A-C) and Rab6A has two isoforms, termed Rab6A and Rab6A′ [90, 116, 117]. Rab6A′ is produced by alternative splicing of the duplicated exon within Rab6A [116]. The sequence of human Rab6A′ differs from that of Rab6A in only three amino acid residues (Val62 → Ile, Thr87 → Ala, and Val88 → Ala) [116]. Both Rab6A and Rab6A′ were similarly detected in the Golgi apparatus and showed similar GTP-binding activity [116, 118]. Although they appear similar, several studies have reported that the two isoforms show partially different function and binding partner [116, 119]. To understand the different biological effects and Rab6/partner specificity between two Rab6A, I overexpressed, purified and crystallized Rab6A′ (Q72L), which is well known GTP-locked form.

His-tag affinity chromatography followed by gel-filtration chromatography produced 90% pure Rab6A′ (Q72L) and no contaminating bands were observed upon SDS-PAGE analysis (Fig. 1A). The calculated monomeric molecular mass of

Rab6A′ (Q72L), including the N-terminal His tag, was 22 000 Da and its elution peak from size-exclusion chromatography suggests that it exists as a monomer in solution (Fig. 1A).

An initial plate-shaped crystal that diffracted poorly was obtained using condition No. 46 of Crystal Screen. Optimization of the crystallization conditions using a range of concentrations of protein, PEG 8000 and calcium acetate and a range of pH values led to better crystals for diffraction (Fig. 1B). The optimized crystals grew to dimensions of 0.2 × 0.2 × 0.1 mm in 3 days.

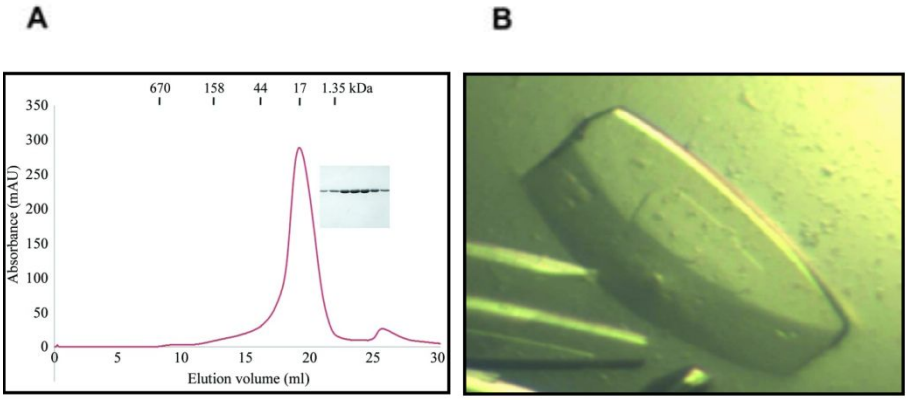

Figure 1. Purification and crystallization of Rab6A′ (Q72L)

(A) Gel-filtration chromatography and SDS-PAGE of Rab6A′ (Q72L). (B) Crystal of Rab6A′ (Q72L). Crystals were grown in 3 days in the presence of 20% PEG 8000, 0.3 M calcium acetate, 0.1 M sodium cacodylate pH 6.7. The approximate dimensions of the crystals were 0.2 × 0.2 × 0.1 mm.

Structure of Rab6A′ (Q72L) complex with GDP/Mg^{2+}

Next, I determined the crystal structure of Rab6A′ (Q72L) at a resolution of 1.9 Å using the coordinates of the previously solved isoform of Rab6A (PDB ID: 2GIL) as the search model for molecular replacement. The asymmetric unit contained two molecules, Chains A and B. The final model contained residues 13–174 for Chain A and residues 12–175 for Chain B (Fig. 2) and one GDP/Mg^{2+} was placed at each chain. The structure was refined to Rwork = 19.6% and Rfree = 25.0%. The overall structure of Rab6A′ (Q72L) showed the typical Ras-like GTPase fold, which was comprised of five α-helices surrounding six β-strands [120] (Fig. 2).

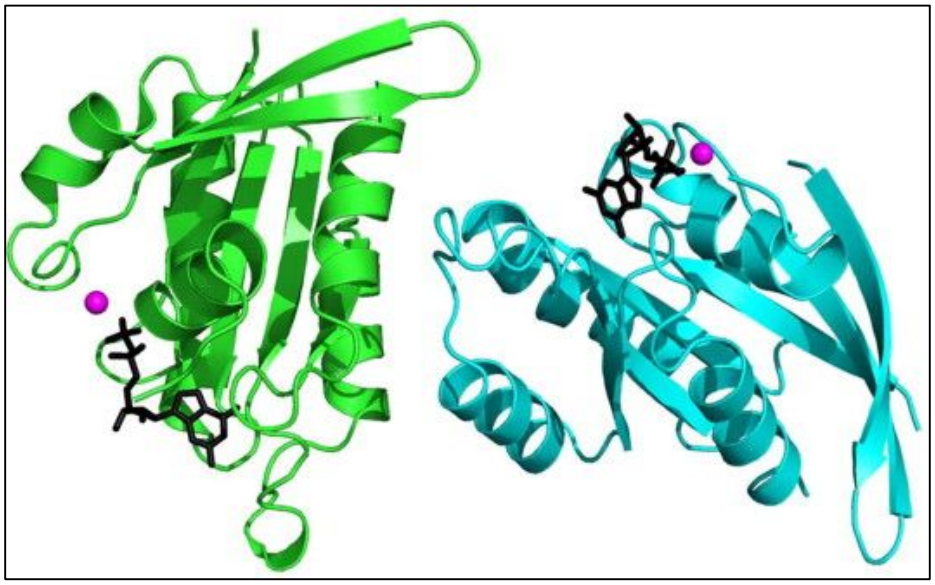

Figure 2. Crystal structure of Rab6A′ (Q72L)−GDP/Mg^{2+}.

Ribbon diagram of Rab6A′ (Q72L)−GDP/Mg^{2+}.

Chain A (Green color) and Chain B (Cyan color) are shown separately. GDP is shown by the black stick. Ball colored in magenta indicates Mg^{2+}.

Unexpectedly located GDP/Mg^{2+}

The Rab6 family has the lowest GTPase activity among the Rab family and Q72L mutant of Rab6A was previously shown to lack GTP hydrolysis activity [113, 121]. Since I thought that they used endogenous GTP and Mg^{2+}, I did not supply any GTP or Mg^{2+} during determination of the structure and expected GTP/Mg^{2+} in the crystal structure of Rab6A′ (Q72L) mutant. However, I found that Rab6A′ (Q72L) contained GDP/Mg^{2+} in the GTP binding pockets, even though it did not have a GTP hydrolysis activity (Fig. 3A and 3B). Mg^{2+} in the Rab6A′ (Q72L) mutant was more closely located to the site where γ-phosphate of GTP was placed in the structure of Rab6A–GTP/Mg^{2+}. The structure of the GDP/Mg^{2+} bound form of Rab6A′ (Q72L) (hereafter referred to as the Rab6A′ (Q72L)–GDP/Mg^{2+}) might have formed due to several possible reasons. First of all, endogenous GDP in the cell can bind to the protein. Because the concentration of GTP in normal cells is much higher than that of GDP, this might be an unusual case. Secondly, GTP bound to the protein may have been hydrolyzed by an unknown factor during purification and crystallization of the protein. Finally, it is possible that GTP can be hydrolyzed

without the active site Q72. Rab6A′ (Q72L) might have a weak activity compared with that of wildtype.

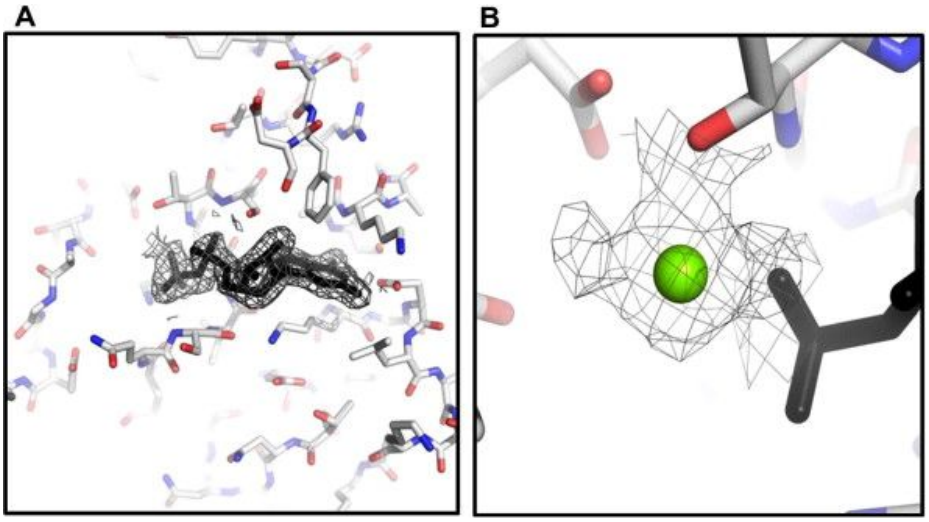

Figure 3. Environment of GDP and Mg^{2+} binding sites.

(A) An omit density map contoured at the 1−σ level around GDP. GDP is shown by the black colored stick and the density map is shown in the gray color. (B) An omit density map contoured at the 1−σ level around Mg^{2+}. Green ball indicates Mg^{2+}. GDP is shown by the black colored stick and the density map is shown in the gray color.

Structural comparison with Rab6A–GTP/Mg^{2+} complex

The human Rab6A–GTP/Mg^{2+} structure was solved in a previous study [113]. The α−carbon atoms of Rab6A′ (Q72L)−GDP/Mg^{2+} was superimposed with those of Rab6A–GTP/Mg^{2+} and the root−mean−square deviation (r.m.s.d.) was 1.5. Pair−wise structural alignments between Rab6A′ (Q72L)−GDP/Mg^{2+} and Rab6A–GTP/Mg^{2+} showed that most parts of the structure were similar except switches I and II, which are critical for controlling the activity of small G protein [122]. The most significantly different region was the orientation of loop in switch II (Fig. 4). One of the interesting features of switch II was the presence of Gln72, which is critical for the hydrolytic activity of Rab6A and Rab6A′ . My structure showed that the side chain of Leu72 was located on the opposite side of Gln72, which caused the loop in switch II to be located in the opposite position (Fig. 4). This indicates that the loss of hydrolytic activity of the Q72L mutant form of Rab6A was likely due to the location of Gln72 (Leu72), which is a critical residue for GTP hydrolysis at small G proteins. In my structure, it was hard to build a model of the switch I region because of the poor quality of the map due to its high flexibility. Based on the disconnected

and poor electron density, a potential model was built and is shown in the Fig. 4 (gray colored dot-box). The structure of switch I might be more close to the open form that was detected in the structure of Mg^{2+}-free and GDP bound form of RhoA (PDB ID: 1DPF), which is also a Ras superfamily of small G protein [122].

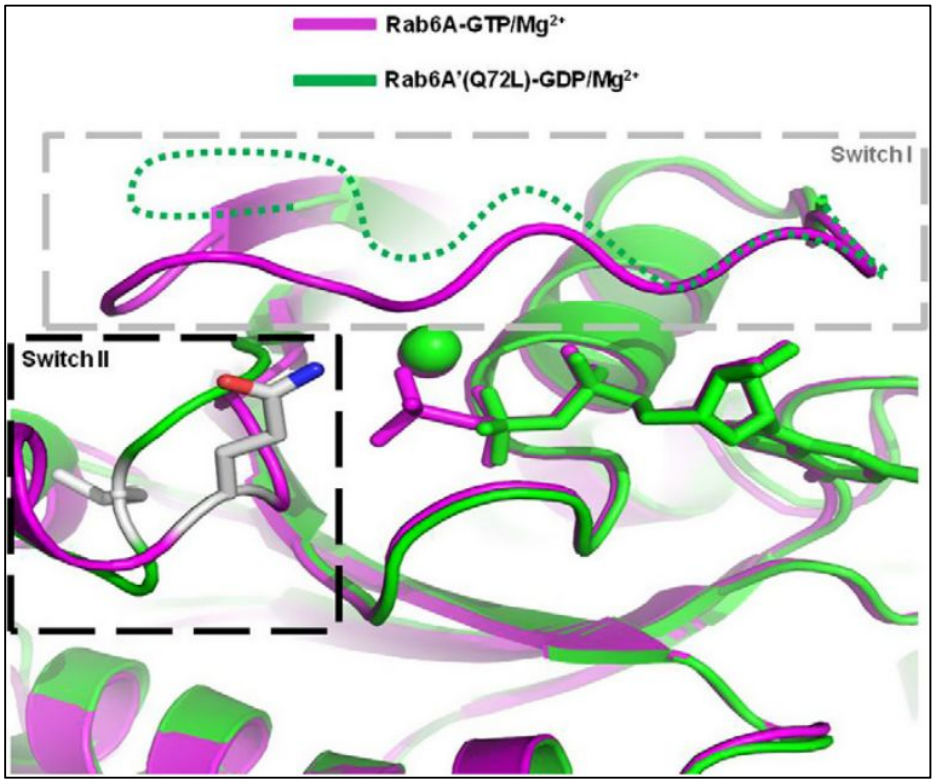

Figure 4. Structural comparison with Rab6A–GTP/Mg^{2+} at the GTP binding domain.

The structures of Rab6A–GTP/Mg^{2+} (PDB ID: 2GIL) and Rab6A′ (Q72L)–GDP/Mg^{2+} (PDB ID: 4KDX) are shown in the magenta and green color, respectively. Gray dot–box and black dot–box indicate switches I and II, respectively. Q72L mutant is shown at the switch II region using a stick representation. Unclear switch I of Rab6A′ (Q72L)–GDP/Mg^{2+}, which is shown with a green dot (model was built with unclear density).

A search of structural homology with the Dali sever

A structural homology search using the DALI server [123] showed that the Rab6A′ (Q72L) mutant has more structural similarity with several different classes of the Ras superfamily of small G protein. The top seven matches, with Z-scores from 27.5 to 25.6, were Rab6 from Plasmodium falciparum [124], Rab6B [125], Rab6A [113], Rab5C [126], SEC4 [127], Rab21 [126], and Rab8A [104] (Table 2). The structural similarity based on the high Z-scores indicates that my structure was more similar with Rab6 from P. falciparum and Rab6B among the same Rab6 family and Rab21 among the same Rab family.

Proteins and Accession ID	Z-score	R.M.S.D(Å)	Identity (%)
Rab6 (1D5C)	27.5	0.8	69
Rab6B (2FFQ)	27.0	1.3	91
Rab6A (2GIL)	26.9	1.5	97
Rab5C (1Z0D)	26.8	1.0	46
SEC4 (1G16)	25.9	1.2	35
Rab21 (1Z08)	25.5	1.3	39
Rab8A (3QBT)	25.4	1.3	44

Table 2. Structural similarity search using DALI server [123].

Mapping of different amino acids between Rab6A and Rab6A′

The sequence of human Rab6A′ differs from that of Rab6A in only three amino acid residues (Val62 → Ile, Thr87 → Ala, and Val88 → Ala) [116]. It has been shown that the two isoforms are functionally different even though they have almost the same amino acids sequence. This functional difference may be caused by their interaction partner. For example, it is well known that Rab6A interacts with Rabkinesin-6 but Rab6A′ does not [116, 119].

Mapping of the three amino acid residues (Val62 → Ile, Thr87 → Ala, and Val88 → Ala) that were different between the two isoform onto the Rab6A′ (Q72L)-GDP/Mg^{2+} surface showed that all three residues were located on the side opposite of the GTP/Mg^{2+} binding site (Fig. 5). Since Rab6A, not Rab6A′, is known to interact with Rabkinesin-6, it is possible that this mapped region of the Rab6A′ (Q72L)-GDP/Mg^{2+} surface might be interaction region with Rabkinesin-6.

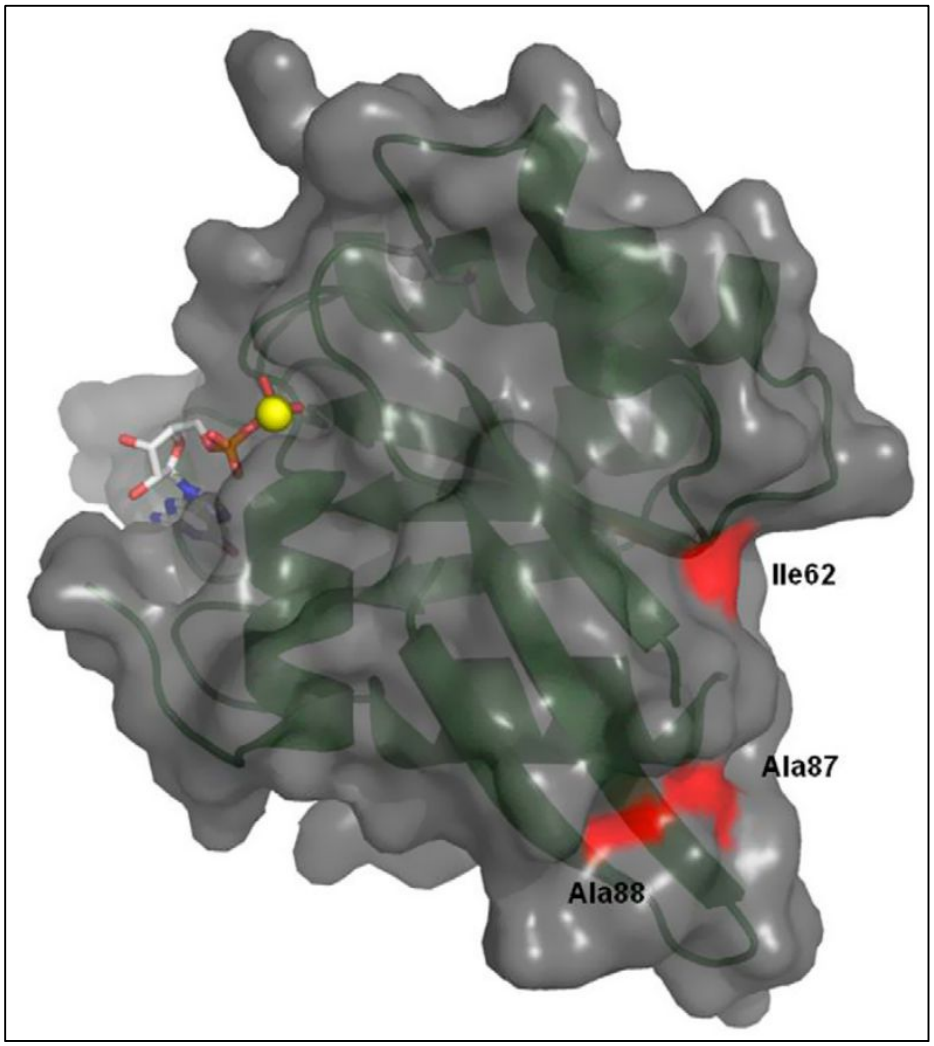

Figure 5. Mapping of different amino acids between Rab6A and Rab6A′ .

Molecular surface is shown in the gray color and different amino acids are marked in the red color. GDP and Mg^{2+} are shown as a stick and sphere, respectively.

DISCUSSION

Although the Q72L mutant has been shown to be in the GTP-lock form, Rab6A′ (Q72L) possesses GDP/Mg^{2+} in the GTP binding pocket, which is formed by a flexible switch I and switch II. It is well known that the Rab6 family has the lowest GTPase activity among the Rab family [113, 121]. Generally, active form of GTPase is turned off by GTP hydrolysis and conserved glutamine on switch II (Q72 in Rab6A family) mediates GTP hydrolysis by stimulating water molecule which is bound to the GTPase and γ-phosphate of GTP. In QL mutant of GTPase (Q72L in Rab6A), the substituted leucine could not stimulate water molecule, thus it maintained active state of protein. Interestingly, the electron density was observed in the vicinity of active site, and I identified that this density was site for water molecule through several times of model refinement by Refmac5 (Fig. 6A) [115]. Based on structural analysis, the location of water molecule in Rab6A′ (Q72L) is identical to that in Rab6A. Next issue is the question that how this water hydrolyzed GTP and which domain or residue participates in water-mediated nucleophilic attack for GTP hydrolysis. Rab6 family has another glutamine on P-

loop and this is exceptional compared to other Rab family (Fig. 6B). In normal Rab6A, this glutamine (Gln-22) is closely located to Gln-72, thus both of two glutamines hardly contact water molecule because of sterically repulsion. In Rab6A′ Q72L, simulation of backbone dependent rotation in Gln-22 revealed that Gln-22 could contact water molecule within 3Å because switch II domain was shifted to outside region away from active site. Taken together, I concluded that the conformational rearrangement of switch II domain was triggered during crystallization, and Gln-22 alternatively activated water molecule for GTP hydrolysis. Despite fortuitous hydrolysis of GTP to GDP was observed, this structure represented inactive form of Rab6A because large conformational changes were detected in switch I and switch II regions which were commonly observed in other inactive GTPases. This structure provides several insights for understanding of functional properties of Rab6A and Rab6A′. First, Rab6A′ could bind to specific binding partner without conformational changes. Despite the three amino acids differ from Rab6A and Rab6A′ (residues at 62, 87 and 88), domain conformations of Rab6A′ between β3-5 strands are identical

to that of Rab6A. In addition, structure of inactive form of Rab6A shows similar overall structure to active form of Rab6A. Although domains in the vicinity of active site are largely rearranged, other regions show similar conformations. Thus, this observation indicates that the effector proteins could bind to conserved region in both active- and inactive states of Rab6A. Indeed, previous study reported that effector protein binds both states of Rab6A. R6IP1 (Rab6-interacting protein 1) is firstly identified as a Rab6-binding protein [128]. In that study, R6IP1 could bind to Rab6A and Rab6A′ , as well as Rab11A [19]. Interestingly, interaction between R6IP1 and Rab6A is independent on nucleotide specificity, while R6IP1 interacts only with active form of Rab11A [19].

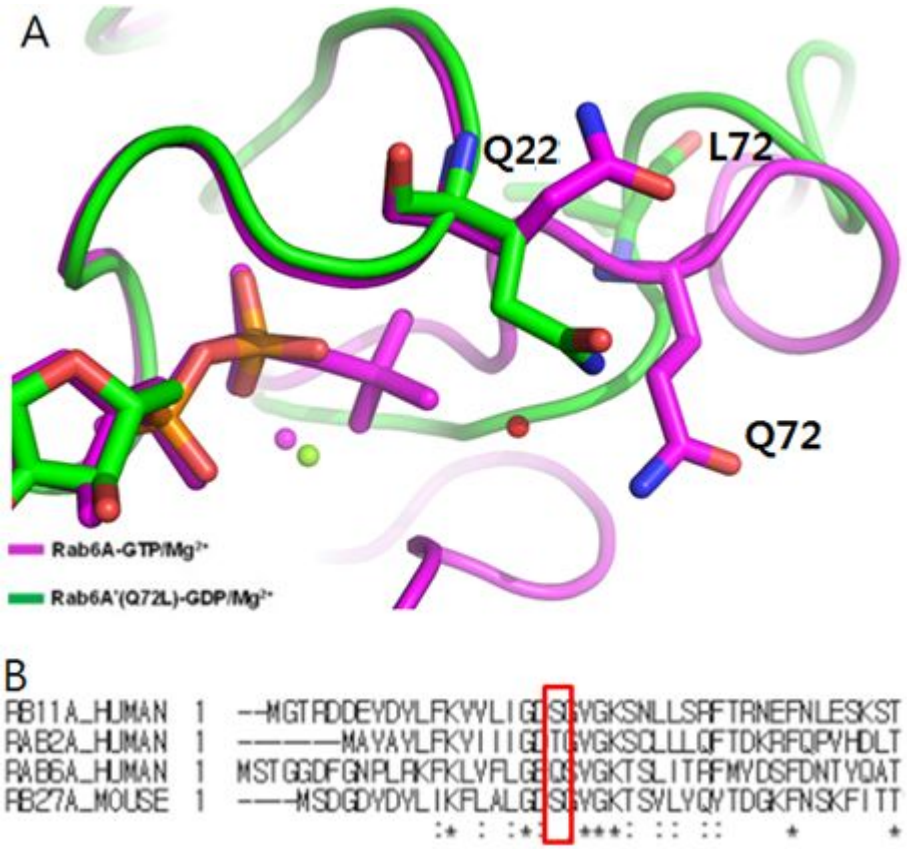

Figure 6. Water molecules in Rab6A′ (Q72L) model.

(A) Electron density revealed the existence of water molecules in protein model. The water molecule (colored as red) was commonly observed in crystal structures of other Rab GTPases which have hydrolysis activity. In addition, Gln-22 of Rab6A′ (Q72L) has closer distance than that of Rab6A. (B) Sequence alignment of Rab family. Phosphate-binding residue of P-loop dlomain is well conserved among GTPases. However, this residue of Rab6 is not conserved exceptionally. Generally, these residues are conserved as serine or threonine.

Rab GTPases regulate their cycle and specific pathways by interacting with regulator proteins and effector proteins, respectively. Although Rab GTPases are similar in their overall structure, binding proteins that regulate their activity and mediate their downstream function are not. Rab regulator proteins such as GAPs and GEFs, recognize conformational change in catalytic domains which are critically affected substrate-bound state. Therefore, they could share several Rab members as binding partner, but they could not bind to both active- and inactive state of one Rab GTPase. However, Rab effector proteins could bind both states of Rab GTPases, if they recognize other domain on Rab GTPase which is not critically affected by substrate bound state. In this point, analyzing the structure and property of Rab6A family provides a unique angle to understand Rab-mediated network but exactly roles what they perform is still needed to investigate in greater detail.

CHAPTER 2

Molecular mechanism of constitutively active Rab11A was revealed by crystal structure of Rab11A S20V

MATERIALS AND METHODS

1. Protein expression and purification

The methods used for expression and purification in this study have been described in detail [129]. Briefly, human Rab11A (S20V), which corresponds to amino acid residues 8–175, was expressed in BL21 (RIPL) E. coli competent cells under overnight induction at 293 K. Human Rab11A (S20V) contained a C-terminal His-tag and was purified by nickel affinity chromatography followed by size-exclusion chromatography over a Superdex 200 size-exclusion column (GE Healthcare, Waukesha, WI, USA) that had been pre-equilibrated with a solution of 20 mm Tris pH 8.0 and 150 mm NaCl. The target protein was concentrated to 14 mg·mL-1.

2. Crystallization and data collection

The crystallization conditions were initially screened at 293 K by the hanging-drop vapor-diffusion method using various screening kits. Initial crystals were grown on plates by equilibrating a mixture containing 1 μL protein solution (14 mg·mL-1 protein in 20 mm Tris pH 8.0, 150 mm NaCl) and 1 μL of reservoir solution containing 2.5 m sodium chloride, 0.2 m

magnesium chloride, and 0.1 m Tris pH 7.0 against 0.3 mL of reservoir solution. Crystals appeared within 5 days and grew to maximum dimensions of 0.1 × 0.1 × 0.1 mm in the presence of 2.4 m sodium chloride, 0.1 m magnesium chloride, and 0.1 m Tris pH 7.1. A 2.4 Å native diffraction data set was collected from a single crystal at beamline BL-4A of the Pohang Accelerator Laboratory (PAL), Pohang, South Korea. The data sets were indexed and processed using HKL2000 [112].

3. Structure determination and analysis

The structure was determined by the molecular replacement phasing method using Phaser [130]. The previously solved structure of GDP-bound Rab11A (PDB code: 1OIV) [131] was used as a search model. Model building and refinement were performed by COOT [114] and Refmac5 [115], respectively. Water molecules were added using the ARP/wARP function in Refmac5. The final model of both chain A and chain B contained residues 8–175. One GTP/Mg^{2+} was placed at each chain. The geometry was inspected using PROCHECK and found to be reasonable [132]. A total of 93.98% of the amino acids were located in the most favorable region and 6.02% were in the

allowed regions of the Ramachandran plot. The data collection and refinement statistics are summarized in Table 1. All molecular figures were generated using the program pymol (The Pymol Molecular Graphics System (2002), DeLano Scientific, San Carlos, CA, USA).

Data collection	Native
Space group	I4
Cell dimensions	
a, *b*, *c*	74.11Å, 74.11Å, 149.44Å
Resolution	50–2.4Å
R_{sym} [a]	12.5% (75.4%)
Mean $I/\sigma(I)$ [a]	30.8 (3.9)
Completeness [a]	100% (100%)
Redundancy [a]	7.5 (7.6)
Refinement	
Resolution	41–2.4Å
No. of reflections used	14 877
R_{work}/R_{free}	22.7%/29.1%
No. of atoms	
Protein	2619
Water and other small molecule	75
Average *B*–factors	44.5 Å^2
R.m.s deviations	
Bond lengths	0.015 Å
Bond angles	1.927°
Ramachandran plot	
Most favored regions	93.98%
Additional allowed regions	6.02%

a Highest resolution shell is shown in parenthesis

Table 1. Crystallographic statistics.

4. Multi-angle light scattering (MALS)

The molar mass of Rab11A (S20V) was determined by MALS. Briefly, highly purified Rab11A (S20V) was injected onto a Superdex 200 HR 10/30 size-exclusion column (GE healthcare) that had been equilibrated with buffer containing 20 mm Tris HCl and 150 mm NaCl. The chromatography system was coupled to a MALS detector (mini-DAWN EOS, Santa Barbara, CA, USA) and a refractive index detector (Optilab DSP) (Wyatt Technology, Santa Barbara, CA, USA).

5. Protein Data Bank accession code

The coordinate and structure factors have been deposited in the Protein Data Bank (PDB) with accession code 5EZ5.

RESULTS

Structure of Rab11A S20V with GTP/Mg^{2+} complex

The Rab11 family is a representative Rab GTPase family involved in the control of TfR recycling and its routing to the exit from recycling endosomes [96, 97]. The functions of the Rab11 family have also been found in various places in the cell, including mobilization of endosomal membranes for phagocytosis in macrophages [98]. Three mutation models of Rab11A that affect GTPase activity have primarily been used to investigate the function of Rab11A (Fig. 1A). In the Rab GTPase family, glutamine in switch II (Q70 in Rab11A) is highly conserved and a major target for the generation of defective mutants for GTP hydrolysis. In this context, Rab11A Q70L has also been used extensively as a putative GTPase-defective mutant. However, Rab11A S20V, not Q70L, has been considered a dominant GTPase-deficient mutant in some cases [64, 133]. To better understand the mutagenesis-based activity control of Rab11A, I purified, crystallized, and determined the crystal structure of defects of the GTP hydrolysis form, GTP-locked, constitutively active form of Rab11A, Rab11A S20V, at a resolution of 2.4 Å using the

coordinates of the previously solved GDP binding form of Rab11A (PDB id: 1OIV) as the search model for molecular replacement. The asymmetric unit contained two molecules, chain A and chain B (Fig. 1B). The final model of both chain A and chain B contained residues 8–175, and one GTP/Mg^{2+} was placed at each chain (Fig. 1B). The structures of the two monomers in the asymmetric unit are nearly identical, having a root−mean−square deviation (RMSD) of 1.12 (Fig. 1C). The structure was refined to an Rwork = 22.7% and Rfree = 29.1%. The overall structure of Rab11A S20V showed the typical Ras−like GTPase fold, which was comprised of four or five α−helices surrounding six β−strands (Fig. 1C) [120].

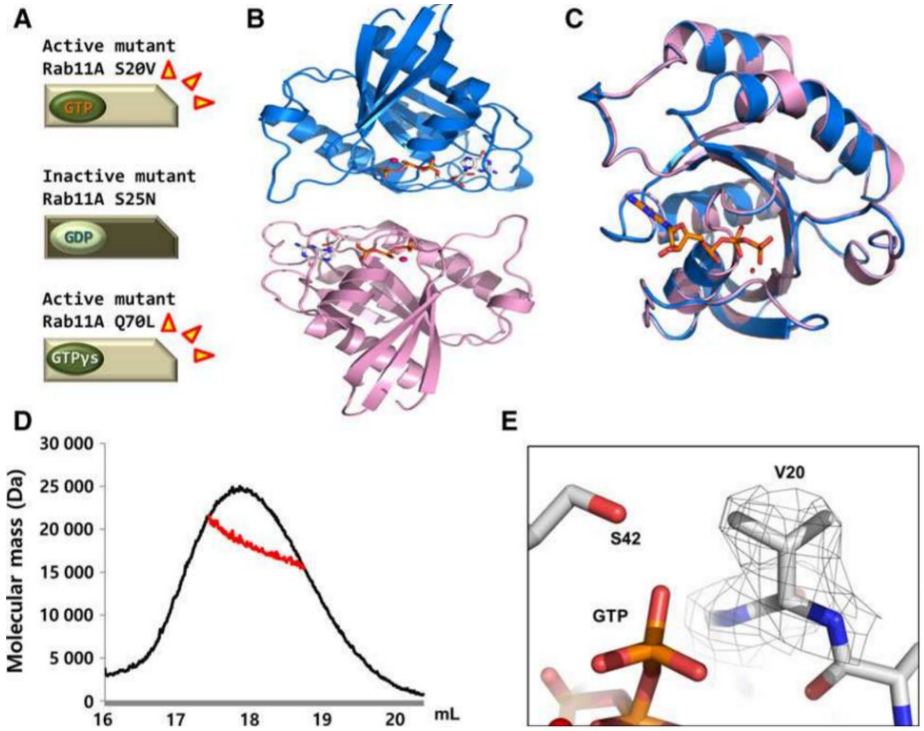

Figure 1. Crystal structure of human Rab11A S20V.

(A) Various mutants of Rab11A were extensively utilized to investigate its function. The mutated Rab11A in the P-loop (S20V) or Switch II (Q70L) was widely used as an active form, while Rab11A S25N mutant was used as a GDP-bound inactive form with defective GTP binding. (B) The overall structure of Rab11A S20V. In the crystals, the asymmetric unit contained two molecules, chain A (blue) and chain B (pink). (C) Superposition of the Rab11A S20V chain A (blue) and chain B (pink). When the two chains were aligned, the rmsd value was

0.15. GTP and Mg^{2+} are drawn as sticks and red spheres, respectively. (D) Determination of the molecular mass of Rab11A S20V by multi-angle light scattering (MALS). The calculated monomeric molecular weight of Rab11A S20V including the C-terminal His-tag was 20.9 kDa, indicating that Rab11A S20V is a monomer in solution. (E) Density map with atomic model showing substitution of S20 to V in the nucleotide binding pocket of Rab11A S20V. Rab11A S20V (green) and Rab11A Wild-type (cyan) are superimposed. An omit density map contoured at the 1-σ level around V20. The density map of Rab11A S20V is shown in black. Only the density map of V20 is shown for better visualization.

Because of the possibility of functional dimeric forms of Rab11A S20V in solution on the basis of the current structure, I calculated the molecular weight using size-exclusion chromatography. The results revealed that Rab11A S20V is a monomer in solution that elutes at around 20 kDa from the size calibrating size-exclusion column (Fig. 2). The accurate molecular weight of Rab11A S20V was confirmed by multi-angle light scattering (MALS), which can detect the absolute molecular weight of the target protein in solution. This experiment also produced the same results as size-exclusion chromatography. The theoretical monomeric molecular weight of Rab11A S20V including C-terminal His-tag (LEHHHHHH) was 20.9 kDa, while that of MALS was 18.8 kDa (0.5% fitting error), indicating that Rab11A S20V is a monomer in solution, similar to other Rab proteins (Figs 1D and 3). These findings indicate that asymmetric dimers are artifacts of crystal packing. On the basis of the electron density map, I confirmed that Ser-20 was correctly substituted to Val at the nucleotide binding pocket of Rab11A S20V (Fig. 1E).

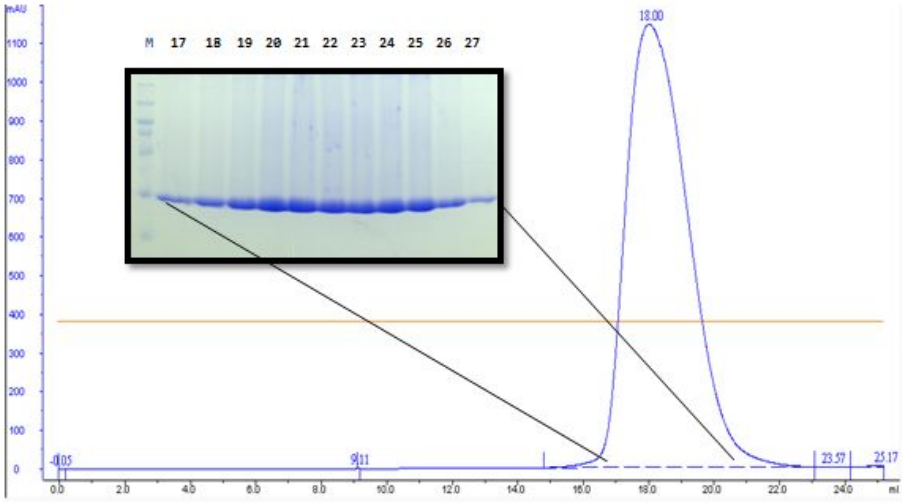

Figure 2. Size exclusion chromatogram and fractions of Rab11A S20V.

The eluted Rab11A S20V was applied onto a Superdex 200 column that had been pre-equilibrated with 20 mM Tris pH 8.0, 150 mM NaCl at 277K

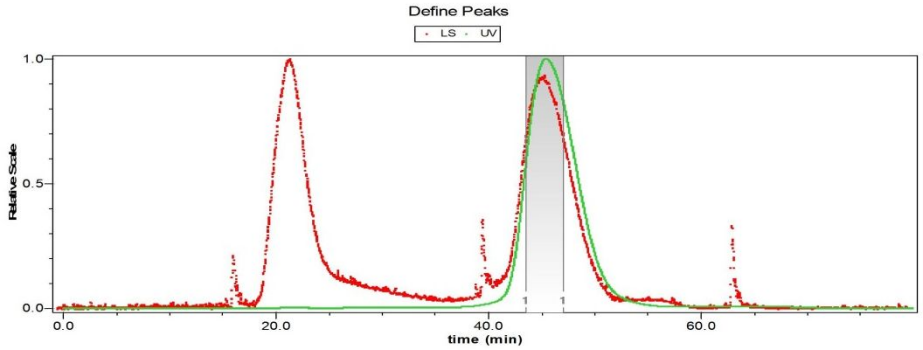

Peak Results	
Calculated Mass (µg)	1405.99
Mass Recovery	n/a
Mass Fraction (%)	100.0
Molar mass moments (g/mol)	
Mn	1.915×10^4 (±1.570%)
Mp	1.861×10^4 (±1.045%)
Mv	n/a
Mw	1.933×10^4 (±1.567%)
Mz	1.952×10^4 (±3.500%)
Polydispersity	
Mw/Mn	1.009 (±2.219%)
Mz/Mn	1.019 (±3.836%)
rms radius moments (nm)	
Rn	12.2 (±31.5%)
Rw	12.6 (±29.5%)
Rz	13.0 (±27.6%)

Figure 3. Raw data of MALS.

The theoretical monomeric molecular weight of Rab11A S20V including C-terminal His-tag (LEHHHHHH) was 20.9 kDa. The calculated molecular weight of Rab11A S20V by MALS was 18.8 kDa.

Endogenous GTP and Mg^{2+} in the GTP binding site of Rab11A

Because of the rapid GTP hydrolysis activity of Rab11A, it has been difficult to trap its active form. Based on biochemical and mutational studies, it is well known that S20 plays an important role in the GTP hydrolysis activity of Rab11A and that S20 substitution to V causes loss or reduced activity. Since I expected Rab11A S20V to use endogenous GTP and Mg^{2+}, I did not supply either during purification and determination of the structure. As expected, GTP and Mg^{2+} were found in the nucleotide binding pocket of Rab11A. Endogenous GTP was not hydrolyzed and was clearly located in the binding pocket in intact form (Fig. 4). Although GDP-bound Rab family members have been found in nucleotide free condition during the purification step [134], the GTP bound current Rab11A structure is not surprising because the concentration of GTP in normal cells is much higher than that of GDP. Residues including G21, K24, S25, N26, S40, S42, T43, G69, K125, and D127 were involved in the hydrogen bond interactions with GTP (Fig. 4). The side chains of S40 and S42 on the previously solved structure of Rab11 complexed with GTPγS did not participate in the interaction with GTPγS [131]. However, my

structure showed that the side chains of S40 and S42 on switch I were flipped 180° and formed hydrogen bonds with α− and γ−phosphate of GTP. These findings indicate that several serines on switch I including S40 and S42 can change the conformation to accommodate many states of nucleotides to control the activity of Rab11A. Mg^{2+} was located at the site at which β− and γ−phosphate of GTP was placed in the structure of Rab11A complexed with GTPγS by coordinating with S25 and T43 (Fig. 4). In previous structures of inactive Rab GTPase, the switch I region was in the opened or mobile state in the absence of GTP and Mg^{2+}. However, Rab11A S20V shows that S40 and S42 on switch I interacts with GTP, and T43 interacts with Mg^{2+}, by which the switch I region is closed (Fig. 4). This closed conformation of the switch I region was commonly observed in the active state of monomeric Rab GTPase.

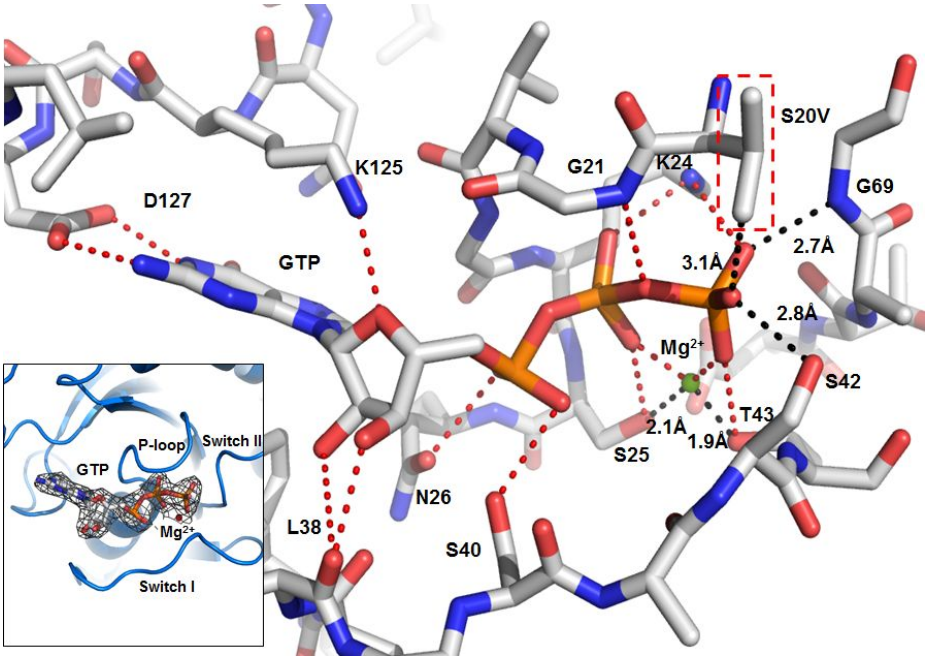

Figure 4. Endogenous GTP and Mg^{2+} interactions with Rab11A S20V.

Magnesium ions found in Rab11A S20V structures are shown as green spheres. Interactions are represented as red- and black-dotted lines. Measured distances between are represented as black-dotted lines. The bottom left shows an electron density map of GTP in Rab11A S20V drawn as a ribbon diagram.

Structural comparison with Rab11A complexed with other nucleotides.

Four structures of Rab11A complexed with different nucleotides, GNP, GDP, GDP + Pi, and GTPγS, are currently available [126, 131, 135]. The α-carbon atoms of three Rab11s were superimposed with those of Rab11A S20V-GTP/Mg^{2+} to compare the structures. The RMSD was 1.70 with GDP complex structure, 0.88 with GDP + Pi complex structure, 0.49 with GTPγS complex structure and 0.27 with GNP complex structure. This superimposition study showed that most parts of the structure were similar, except switch I and II, which are critical to controlling the activity of small G protein [122]. Switch I and II are relatively conserved in the GNP complex, GTP complex, GTPγS complex, and GDP + Pi complex, while those of GDP complex are out-fitted, indicating that switch I and II are the most dynamic structures on Rab11A (Fig. 5). The locations of each nucleotide in the pocket are slightly different. However, the overall orientations of nucleotides were almost identical, except in the case of the Rab11A-GDP + Pi complex. Hydrolyzed γ-phosphate was tilted to switch II in the structure (Fig. 5).

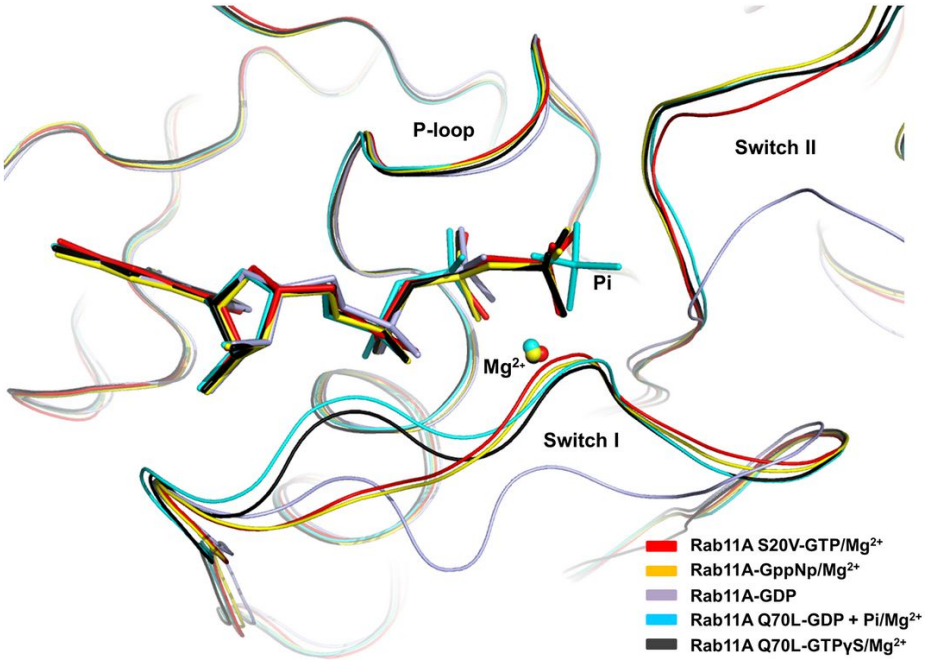

Figure 5. Structural comparison of Rab11A complexed with other nucleotides at the GTP-binding domain.

The structures of Rab11A S20V-GTP/Mg^{2+}, Rab11A-GppNp/Mg^{2+} (PDB ID: 1YZK), Rab11A-GDP (PDB ID: 1OIV), Rab11A Q70L-GDP + Pi/Mg^{2+} (PDB ID: 1OIX), and Rab11A Q70L-GTPγS/Mg^{2+} (PDB ID: 1OIW) are shown in red, yellow, light blue, cyan, and black, respectively. Magnesium ion, which is indicated by spheres, was observed in most structures of Rab11A except that of Rab11A-GDP (light blue).

Structural similarity search using DALI.

A structural homology search using the DALI server [123] showed that Rab11A S20V has more structural similarity with several different classes of the Ras-superfamily of small G protein. The top five matches, which had Z-scores from 15.2 to 12.3, were Rab11B (Isoform of Rab11), Rab25, Rab1B, Rab1A, and Rab8A (Table 2).

Proteins and accession ID	Z-score	RMSD (Å)	Identity (%)	References
Rab11B (2F9M)	15.2	0.55	92	[136]
Rab25 (3TSO)	15.2	0.83	71	Not Published
Rab1B (3NKV)	13.7	0.95	53	[137]
Rab1A (4IRU)	12.3	1.07	51	[138]
Rab8A (3GBT)	13.9	0.96	47	Not published

Table 2. Structural similarity search using DALI.

Structural basis for the GTPase activity of Rab11A S20V compared to other Rab11As.

The results of my previous study showed that the backbone structure of the P-loop is unaffected by substitution of S20 to V. In addition, the overall structures of GTP- or GTP analogue-bound Rab11A are very similar (Fig. 5). Since the P-loop and switch I/switch II are known to be critical for GTP/GDP binding and the function of GTPase activity, I further compared the side chain orientations of three regions between Rab11As to provide a detailed explanation of the distinct characteristics of Rab11A S20V.

Comparison of individual amino acid orientations in Rab11A and its mutants revealed interesting differences between Rab11A S20V and other Rab11As (Fig. 6). Rab11A WT and Rab11A S20V possess a similar switch I and switch II. The side chains of S40 and S42 on switch I of both structures interact with α- and γ-phosphate of GTP, respectively (Fig. 6A, C). In contrast, the side chains of those amino acids on switch I of Rab11A Q70L are oriented in the opposite direction away from GTPγS (Fig. 6B). Interestingly, L70 on switch II was closely associated with R72 in Rab11A Q70L, with a distance of 3.0 Å

(Fig. 6B). Next, I compared the side chain orientations at residue 20 on the P-loop. Not surprisingly, the side chain orientations differed since the three structures consisted of different combinations of 20- and 70-residues (Fig. 6A-C). I further investigated whether there were other differences with significant implications around this region. Several groups have previously reported that GTP hydrolysis of GTPase depends on the location of the water molecule because the side chain of glutamine on switch II hydrolyzes GTP by activating nucleophiles that attack water molecules [139, 140]. Figure 6D shows the occupation of water molecules in Rab11A WT, Rab11A S20V, and Rab11A Q70L. In all structures, two water molecules were observed around Mg^{2+}, which interacts with GTP, S25, and T43 (Fig. 6D). However, the water molecule located between γ-phosphate of GTP and residue 70 on switch II is present in Rab11A WT and Rab11A Q70L, but absent from Rab11A S20V (Fig. 6D). Since this water molecule is known to be activated by switch II to hydrolyze GTP to GDP + Pi, I further measured the electron density to identify water molecules around this region. Searching for electron densities under the 0.8-σ level revealed no water molecules around this

region (Fig. 6E). This observation is believed to reflect a larger side chain of V20 that sterically interferes with localization of the water molecule. Supporting my observations, an early in vitro study showed consistent differences between GTPase activities of Rab11A S20V and Rab11A Q70L. GTP-binding analysis revealed that Rab11A Q70L had attenuated GTPase activity, but GTP could be hydrolyzed to GDP + Pi via activation of GAP [133]. This result might be explained by the nucleophilic water molecule not being activated by L70 on switch II of Rab11A Q70L because of the chemical properties of leucine, while it could be stimulated by GAP activation. In contrast, Rab11A S20V did not exhibit intrinsic and GAP-stimulated GTPase activity. Therefore, my observations indicate that the larger V20 appears to interfere with proper localization of the water molecule, which mediates nucleophile attack of the γ-phosphate of GTP, resulting in GTP being locked in an active form of Rab11A S20V.

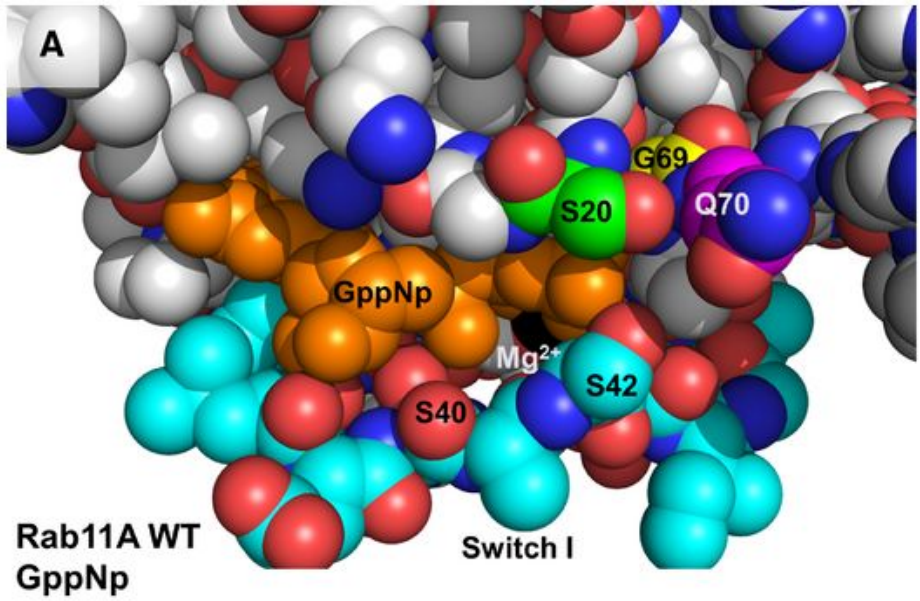
A
G69
S20
Q70
GppNp
Mg2+
S42
S40
Rab11A WT
GppNp
Switch I

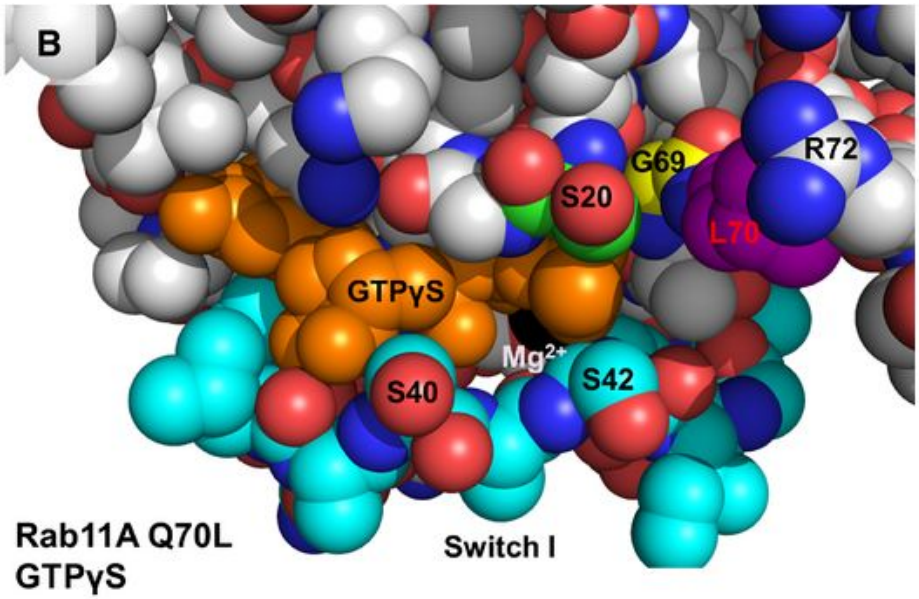
B
G69
R72
S20
L70
GTPγS
Mg2+
S40
S42
Rab11A Q70L
GTPγS
Switch I

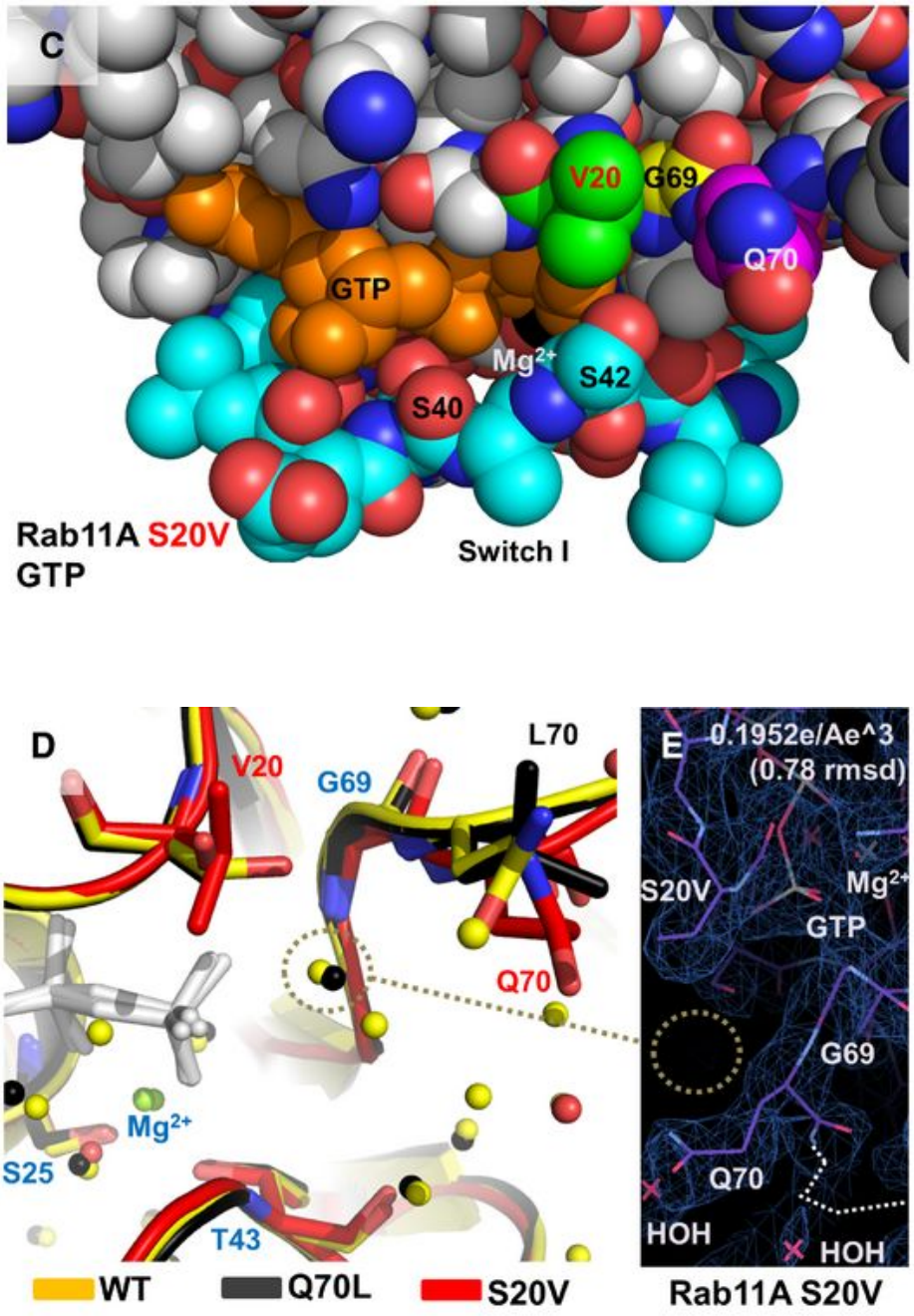

Figure 6. Features of the structures of Rab11A WT, Rab11A Q70L and Rab11A S20V.

(A-C) Space filling model showing the surface at the guanine nucleotide pocket of Rab11A WT (A), Rab11A Q70L (B) and Rab11A S20V (C). The colors of the switch I region, guanine nucleotide and Mg^{2+}, are cyan, orange, and black, respectively. Rab11A WT and Rab11A S20V possess similar switch I and switch II and differ from Rab11A Q70L, which possess mutated switch II. (D) The location of water molecules around the GTP-hydrolysis region. Rab11A WT (yellow), Rab11A Q70L (black) and Rab11A S20V (red) are superimposed. Water molecules are observed in the GTP-hydrolysis region of Rab11A WT (yellow) and Rab11A Q70L (black). In Rab11A S20V (red), water molecules are observed around Mg^{2+} like other Rab11As, but not around the GTP-hydrolysis region. (E) The electron density map of Rab11A S20V shows that water molecules are not measured around the GTP-hydrolysis region in Rab11A S20V.

DISCUSSION

The phosphate-binding loop (P-loop) is one of the essential motifs for GTP hydrolysis activity in GTPase. In Ras GTPase, the P-loop contains G12, which is a target for G12V mutation [141]. It has been previously reported that Ras G12V possesses a weak GTPase activity, resulting in a GTP-bound state [142]. In contrast, the structure of Rac2 G12V was resolved in a GDP-bound state [143]. It has also been reported that Giα1 G42V, which is analogous to Ras G12V, showed attenuated GTPase activity. However, this mutant was not in the GTP-locked form. Interestingly, P-loop mutations among Rab GTPase displayed different results. Occasionally, these mutants lost their GTPase activity when they contained GDP in the active site [144]. In contrast, Rab11A S20V and Rab25 S21V have been observed in the GTP-bound state upon in vitro GTP-binding assay [133]. Taken together, these findings indicate that GTPase activity and GTP affinity in P-loop mutants might occur in a protein-type dependent manner. Generally, most mutants in catalytic region of GTPase have been constructed by sequence alignment from other GTPases which are already known to be active form by structural study

or biochemical study. Therefore, functional activity and molecular mechanism of these mutants must be validated by biochemical analysis and structural analysis. Previously, biochemical analysis of Rab11A and its mutants revealed that constitutively active form of Rab11A is not Q70L but S20V [109]. However, molecular mechanism of Rab11A S20V based on structural analysis has been not yet elucidated.

Rab11A is the most studied gene in Rab family and it is well known that Rab11A plays important role in cellular trafficking by interacting various partners. Here, I present the structure of Rab11A S20V which is known as GTPase-deficient mutant. My result showed distinct features of Rab11A S20V from wild-type and Q70L, based on molecular level by structural analysis. This is the first structure of monomeric Rab11A complexed with endogenous GTP. Furthermore, this is firstly validated by structural analysis for P-loop mutation in human Rab GTPases. My structure showed that substituted V20 of Rab11A interferes with proper localization of a functionally important water molecule, resulting in GTP being locked in an active form of Rab11A S20V.

Referred above in chapter 1, R6IP1 could bind to Rab6A and Rab6A′ , as well as Rab11A but interaction between R6IP1 and Rab6A is independent on nucleotide specificity, while R6IP1 interacts only with active form of Rab11A [19]. Thus I compared three structures for finding of structural diversity between Rab11As and Rab6As (Fig. 7). Superposition of structures between active- and inactive form of Rab11As revealed that Rab11As showed different conformation in several regions depend on substrate binding state. In addition, β6 and β4 strands domain in active Rab11A is rather similar to Rab6A′ than inactive Rab11A (Fig. 7A and 7B, respectively). Interestingly, β4 strand of active Rab11A showed identical conformation to both active form and inactive form of Rab6A (Fig. 7B). I could not say this region is critical to R6IP1 binding, however this result indicates different member of Rab could show similar structure rather than different state of same Rab.

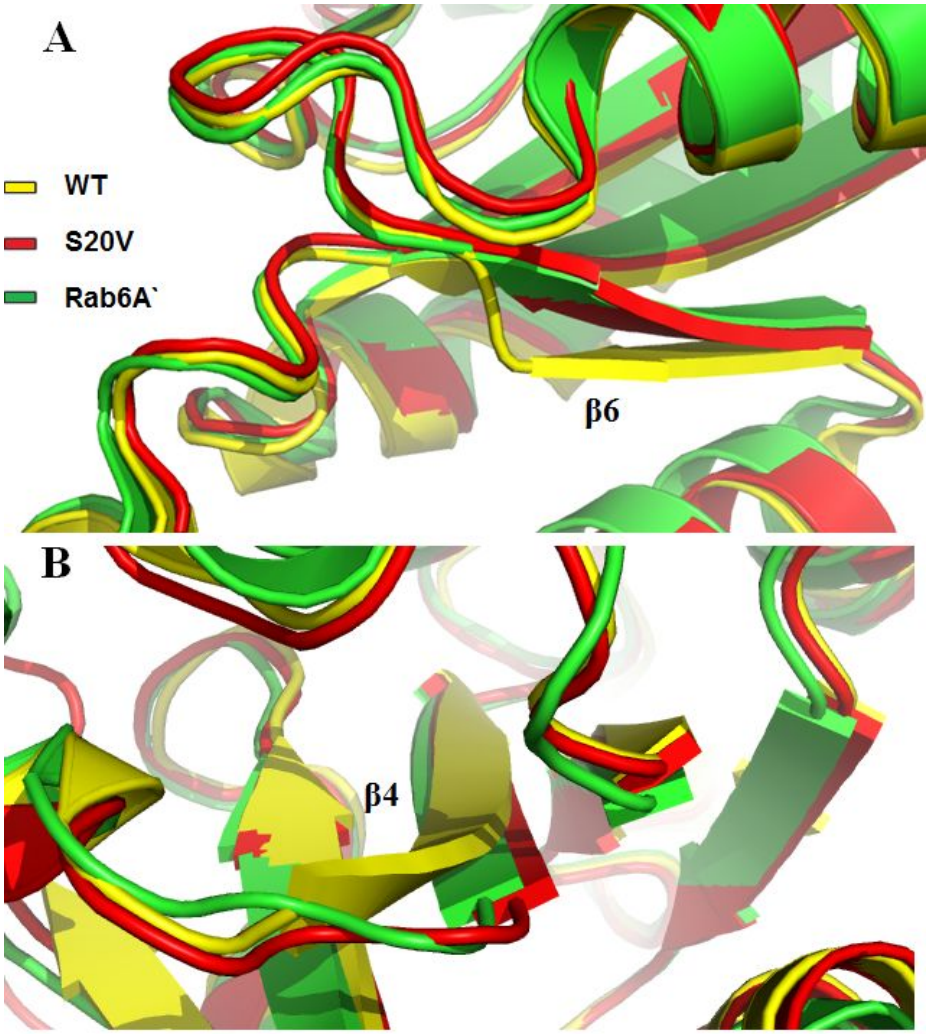

Figure 7. Structural comparison of Rab11As and Rab6A′ Q72L

Structural comparison of wild type of Rab11A, active Rab11A (S20V) and Rab6A′ Q72L. Zoomed up view of β6 strand region (A) and β4 strand region (B).

CHAPTER 3

Occupation of nucleotide in the binding pocket is critical to the stability of Rab11A

MATERIALS AND METHODS

1. Construct design and mutagenesis

Human Rab11A Rab11A Q70L was kindly provided by Dr. Heo, KAIST, Korea. Rab11A Q70L was amplified by PCR using 5′ BamHI and 3′ XhoI overhangs, after which the amplified fragments were inserted into pET15b, resulting in the N-terminally His-tagged Rab11A Q70L (1-173, 19 kDa). To generate wild type Rab11A and various mutants, site-directed mutagenesis was performed using the Quickchange kit (Stratagene) following the manufacturer's protocols. The template used for reverse mutagenesis was pET15b-Rab11A-Q70L, and further mutagenesis was performed using Rab11A as a template. Mutagenesis was confirmed by sequencing.

2. Expression and purification

Plasmids of Rab11A containing wild type and various mutants (Rab11A S20V, S25N and Q70L) were transformed into Escherichia coli BL21 (DE3)-RIPL competent cells (Novagen, USA), after which their expression in LB medium (Rab11A S25N was expressed in both LB and TB medium) was induced

by treatment with 0.5 mM isopropyl β-d-1-thiogalactopyranoside (IPTG) overnight at 293 K when the OD600nm reached 0.65–0.7. Around 5–6 g wet weight of Cells expressing Rab11A and its mutants (Rab11A S20V, S25N, Q70L) were collected, resuspended and lysed by sonication in 20 ml lysis buffer (20 mM Tris pH 8.0, 500 mM NaCl, 25 mM imidazole) supplied with phenylmethanesulfonyl fluoride (PMSF). The lysate was then centrifuged at 16,000 rpm for 30 min at 277 K, after which the supernatant fractions were incubated with 200 ul Ni-NTA beads (Qiagen) for 4 h at 277 K and applied onto a gravity-flow column (BioRad). Next, the unbound bacterial proteins were removed from the column using 100 ml washing buffer (20 mM Tris buffer pH 8.0, 500 mM NaCl, 25 mM imidazole), after which the target proteins were eluted from the column using elution buffer (20 mM Tris buffer pH 8.0, 500 mM NaCl, 250 mM imidazole). The elution fractions were collected as 0.6 ml volumes to a total volume of 3 ml. Fractions containing greater than 80% homogeneous target protein upon SDS-PAGE analysis were then selected and combined. In the final purification step, collected samples were applied onto a size-exclusion chromatographic column

(Superdex-200 10/300, GE Healthcare) that had been pre-equilibrated with FPLC buffer (20 mM Tris buffer pH 8.0 and 150 mM NaCl). The method used to purify Rab11A S25N with GDP is described in Materials and Methods section 6.

3. Solubility assay

The general strategy for the solubility assay was based on the method introduced by Bondos and Bicknell [145]. To investigate the effects of GDP on the solubility of Rab11A S25N, I performed Ni-NTA affinity purification using binding buffer, wash buffer and elution buffer (described in Materials and Methods Section 2) with 200 μM GDP (Binding (+), Washing (+) and Eluting (+), respectively) or without 200 μM GDP (Binding (-), Washing (-) and Eluting (-), respectively). Differently purified samples were incubated at 298 K for 20 min. A total of 400 μl of each 500 μl was utilized for turbidity assay. Turbidity of each sample was directly measured based on the optical density at 600 nm using a spectrophotometer (Beckman). Next, the remaining 100 μl of each sample was utilized for aggregation assay. After centrifugation at 16,000 g

and 277 K for 20 min, each supernatant was assessed by SDS PAGE and Bradford assay (BioRad, Richmond, CA, USA).

4. Native-PAGE assay

Conformational changes in Rab11A S25N with or without GDP were evaluated by native (non-denaturing) PAGE conducted on a PhastSystem (GE Healthcare) with pre-made 8–25% acrylamide gradient gels (GE Healthcare). Coomassie Brilliant Blue was used for staining and detection of the band patterns. Rab11A S25N that had been purified by Ni-NTA chromatography was applied to the gel. The method of Ni-NTA chromatography was described above (see Materials and Methods Section 3). Addition of GDP or Mg^{2+} was performed at the final elution step. Conformational changes in Rab11A were evaluated based on the patterns of the protein bands.

5. Isolation of non-covalently bound nucleotide from protein

Anion exchange chromatography was conducted to isolate nucleotides from Rab11A S25N. First, I collected FPLC fractions of Rab11A S25N that did not overlap with the fraction

of GDP. Before being subjected to anion exchange chromatography, the purified Rab11A S25N was heated at 373 K for 10 min to release the nucleotides from the protein. Denatured protein was then removed by centrifugation at 16,000 g for 30 min at 277 K, after which supernatant was applied to a Mono Q ion-exchange column (GE Healthcare) using starting buffer (20 mM Tris pH 8.0) and elution buffer (20 mM Tris pH 8.0, 1 M NaCl). Next, 1 mM of GDP with 20 mM Tris pH 8.0 and 150 mM NaCl was applied to a Mono Q ion-exchange column (GE Healthcare) using starting buffer (20 mM Tris pH 8.0) and elution buffer (20 mM Tris pH 8.0, 1 M NaCl).

6. Purification and concentration of Rab11A S25N

Briefly, GDP was added into binding buffer, washing buffer and elution buffer to give a final concentration of GDP of 200 μM. Rab11A S25N that had been mixed with 200 μM GDP was then applied onto a size-exclusion chromatographic column (Superdex-200 10/300, GE Healthcare) that had been pre-equilibrated with FPLC buffer (normal buffer was 20 mM Tris buffer pH 8.0, 150 mM NaCl, and 50 μM GDP; acidic buffer was

20 mM sodium citrate at pH 5.0 and 150 mM NaCl, 50 μM GDP). The protein was concentrated to 6–8 mg/ml using Amicon ultra (Millipore).

7. Mutant modeling

The three-dimensional structures of Rab11A wild type and Q70L were publicly available [131], but the three-dimensional model of Rab11A S25N was not available in the protein database at this time. I used the crystal structure model of human Rab11A (PDB ID: 2F9L) as a template of mutant modeling [136]. The serine 25 residue in Rab11A was computationally mutated to asparagine. Possible directions of the mutated residues were modeled based on other GDP bound forms of Rab protein (PDB ID: 3SFV). PyMol software was used to alter the amino acid residues.

RESULTS

Expression and purification of Rab11A and its mutants

I performed site-directed mutagenesis to generate mutants of Rab11A. First, N-terminal tagged 6XHis-Rab11A (1–173) was constructed from Rab11A Q70L and mutated back to wild type. The residue on serine at position 20 in the wild type of Rab11A was then mutated to valine to generate GTP-bound mutant (Rab11A S20V), while the residue on serine at position 25 in wild type was mutated to asparagine to generate GDP-bound mutant (Rab11A S25N). As a result, I obtained four types of Rab11A, including three different types of mutants. Rab11A S20V and Rab11A Q70L mutants have been reported to be GTP- or GTP analog-bound active forms [105, 146]. Each location of mutation in Rab11A S20V and Rab11A Q70L is part of a region known as the P-loop domain and switch II domain, respectively (Fig. 1A). On the other hand, Rab11A S25N mutant has been reported to be a GDP-bound inactive form that is unable to undergo GTP binding [97, 147]. The location of mutation in Rab11A S25N is also described in Fig. 1A. I initially investigated the expression level of the target proteins for the structural and biochemical study of Rab11A and their mutants

(Rab11A S20V, S25N and Q70L). Quantitative analysis of protein eluted from the Ni-NTA affinity column based on Bradford assay and SDS-gel staining showed that all types of Rab11A were highly expressed (Fig. 1B). However, I observed severe precipitation with eluted fractions from Rab11A S25N, unlike other mutants and wild types that are stable at room temperature. I next performed size-exclusive chromatography (SEC) after removing the precipitate by centrifugation. Following FPLC, the intensities of the major peaks of most types of Rab11A proteins were high. In contrast, Rab11A S25N showed low peak intensity (Fig. 1C). These findings fit well with my observation that 1) Ni-NTA eluted fractions of Rab11A S25N became severely turbid at room temperature and 2) the amount of pellet in Rab11A S25N was markedly higher than those of other Rab11As before FPLC injection. Moreover, I observed that Ni-NTA-eluted Rab11A S25N was also precipitated by incubation at 277 K within a couple of hours, indicating that temperature is not the major cause of the low stability of Rab11A S25N.

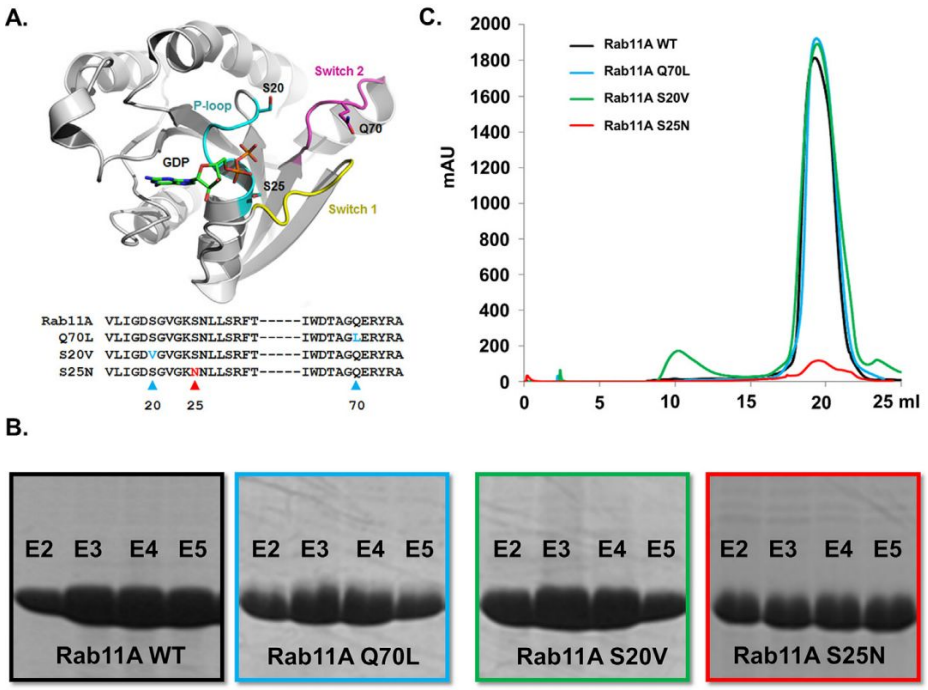

Figure 1. Expression and purification of recombinant Rab11A and its mutants.

(A) Mapping of residues which are involved in guanine nucleotide interaction are shown as stick representations on the catalytic domain of Rab11A. The structural model was produced based on the X-ray structure of GDP-Rab11A (PDB ID: 1OIV). Colored residues in below table indicate the introduced amino acid substitution. (B) SDS PAGE gels of wild type, Q70L, S20V and S25N after Ni-NTA affinity chromatography purification. E (number) indicates elution fraction number. All types of Rab11A were highly expressed. (C) Gel filtration

chromatogram of Rab11A and its mutants. Each sample (Fig. 1B) was injected to FPLC after removing insoluble pellet.

GDP is important to the stability of Rab11A S25N

In the GTPase cycle, it is well known that the release of Mg^{2+} from GTPase leads to the release of GDP [148, 149]. A previous study revealed that the addition of micro-to millimolar levels of Mg^{2+} blocked the release of GDP from wild type Rab [150]. Interestingly, the addition of Mg^{2+} did not block the release of GDP from the inactive form of Rab [150]. It has been reported that mutated residue on the GDP bound form of GTPase perturbs coordination of Mg^{2+} [150, 151]. This perturbation reduces the affinity for GTP, resulting in a GDP-bound state [151]. In this context, I assumed that Rab11A S25N may have a high tendency to release the GDP because of deficient Mg^{2+} binding, resulting in its becoming an unstable protein. I hypothesized that saturation of the GDP-release may solve the instability of Rab11A S25N and speculated that the addition of excessive amounts of GDP to Rab11A S25N instead of the addition of Mg^{2+} may saturate the GDP binding, resulting in high stability. Therefore, I examined the effects of GDP on the stability of Rab11A S25N. Fig. 2A shows the turbidity of Rab11A S25N purified by Ni-NTA chromatography. As expected, proteins purified using elution buffer without GDP

(tube I and tube II) were highly precipitated, while little precipitation was observed in samples that had been purified by GDP containing elution buffer (tube III and tube IV). Interestingly, the least precipitation was observed when I added GDP into all buffer for purification of protein (tube IV), and this state was maintained for over an hour. Similar experiments with other nucleotides (GTP, ATP and ADP) were also conducted, but the degree of precipitation was similar to that of tube I, with no improvement in the solubility of the samples.

To investigate the effects of GDP on Rab11A S25N in greater detail, I conducted a solubility assay. Specifically, I measured the degree of precipitation of Rab11A S25N based on the optical density at 600 nm using a spectrophotometer (Fig. 2B). Consistent with the results previously shown in Fig. 2A, samples eluted by GDP-containing buffer in group III and group IV were less precipitated than those in group I and group II (Fig. 2B). Moreover, the total protein concentration (blue bar) in group III was similar to that in group I and less than that in group II (Fig. 2B). These results could be explained by group I and group III losing more protein during Ni-NTA incubation because non-GDP containing buffer was used (see Binding (-)

in Fig. 2A). The total protein concentration (blue bar) in group II was lower than that in group IV (Fig. 2B) because group II lost more protein during the washing step, which was performed using non-GDP containing buffer (see Washing (-) in Fig. 2A). These findings demonstrated that the GDP affects the solubility and stability of Rab11A S25N in every step during Ni-NTA purification. To confirm that the precipitants corresponded with Rab11A S25N, I conducted SDS-PAGE (Fig. 2C). Additionally, I conducted native gel electrophoresis to investigate whether GDP affected structural changes in Rab11A S25N. As shown in Fig. 2D, the addition of GDP and Mg^{2+} did not alter band position, indicating that GDP and Mg^{2+} did not affect structural changes and the improvement of the stability of Rab11A S25N by GDP was not via structural changes.

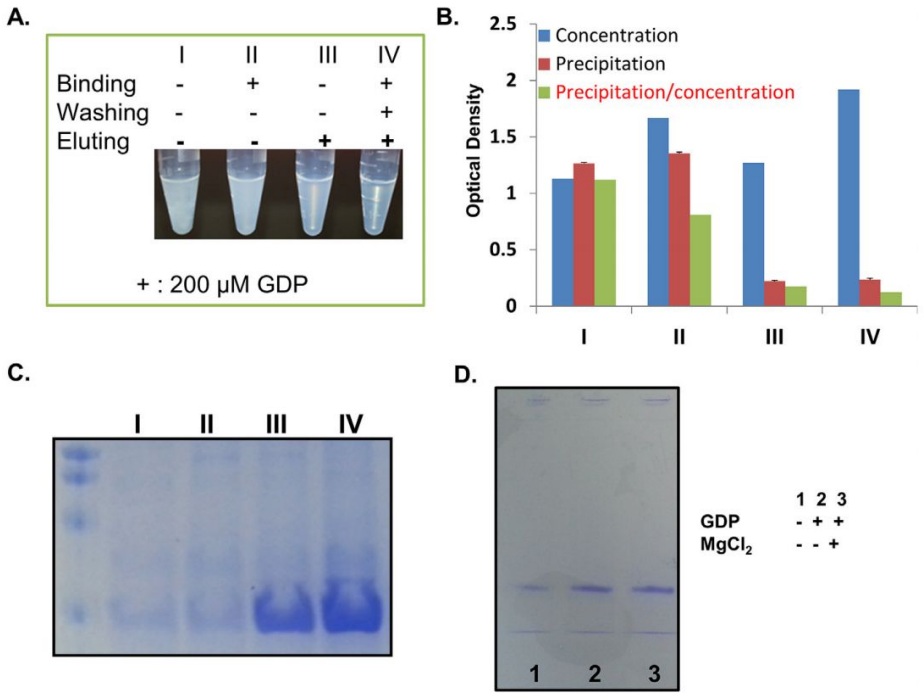

Figure 2. GDP affects the solubility of Rab11A S25N.

(A) Solubility assay was performed to analyze the effect of GDP on Rab11A S25N. (−) indicates absence of GDP in binding buffer, washing buffer or eluting buffer, and (+) indicates 200 μM of GDP was added to buffer. (B) GDP affects precipitation of Rab11A S25N. Turbidity analysis of differently purified Rab11A S25N. Among 500 μl of each sample from Fig. 2A, 400 μl was used for turbidity assay. Blue bar indicates the concentration of eluted Rab11A S25N assessed by Bradford assay (595 nm absorbance). Red bar indicates the turbidity of Rab11A S25N which were incubated at room temperature for

20 min. Green bar indicates the concentration values that are divided by concentration. (C) SDS gel data demonstrated that the precipitated protein was Rab11A S25N. Precipitants in each tube were removed by centrifugation and then supernatant were used for SDS-PAGE. Coomassie brilliant blue was used for staining and detection of bands appeared on the acrylamide gels. (D) GDP affects the solubility of Rab11A S25N without conformational change. Native gel electrophoresis shows that the position of the protein band was not significantly changed.

Occupation of the GDP is critical to the stability of Rab11A S25N

My previous results showed that GDP affects the solubility and stability of Rab11A S25N, but this did not change the structure of Rab11A S25N. To rule out the possibility of non-specific effects of GDP on Rab11A S25N, I examined whether soluble Rab11A S25N contains GDP or not. Since Rab11A S25N and GDP co-existed in the sample eluted from Ni-NTA affinity chromatography, I performed size-exclusion chromatography analysis. The results revealed that excess GDP was separated from Rab11A S25N (Fig. 3A). I then boiled Rab11A S25N (former fractions in Fig. 3A) and centrifuged it to extract GDP from the proteins. After removing the denatured fragments, transparent extract was applied onto a SEC column. I found that this extract was eluted from areas that corresponded exactly to where the excess GDP was (data not shown). It is well known that the electric conductance value of GDP and other nucleotides differs [152], which enabled me to confirm the results of SEC. Therefore, I conducted anion exchange chromatography to compare the electric conductance value of pure GDP and extracts from denatured Rab11A S25N. I found

that the extracts from denatured Rab11A S25N were eluted with the same fraction as pure GDP (Fig. 3B), indicating that GDP affects the protein stability of Rab11A S25N by binding to protein.

After SEC purification, I noticed that purified protein in the major fraction was also precipitated. This might have occurred because GDP was released from Rab11A S25N during the SEC experiments. These findings indicate that Rab11A S25N had a tendency to release the GDP with low affinity for GDP. To maintain the concentration of free GDP during chromatography, I added GDP to the FPLC buffer, which improved protein stability and protected protein from precipitation after purification (Fig. 3C). I also purified Rab11A S25N in acidic buffer with 20 mM sodium citrate at pH 5.0, 150 mM NaCl and 50 μM GDP (Fig. 3D), as well as in high salt buffer condition 20 mM Tris at pH 8.0, 1M NaCl and 50 μM GDP (data not shown). These samples had high purity and were not precipitated after freezing with liquid nitrogen and thawing. Based on these findings, I concluded that saturation of the GDP binding to Rab11A S25N maintains protein stability and is not highly dependent on buffer conditions that were tested.

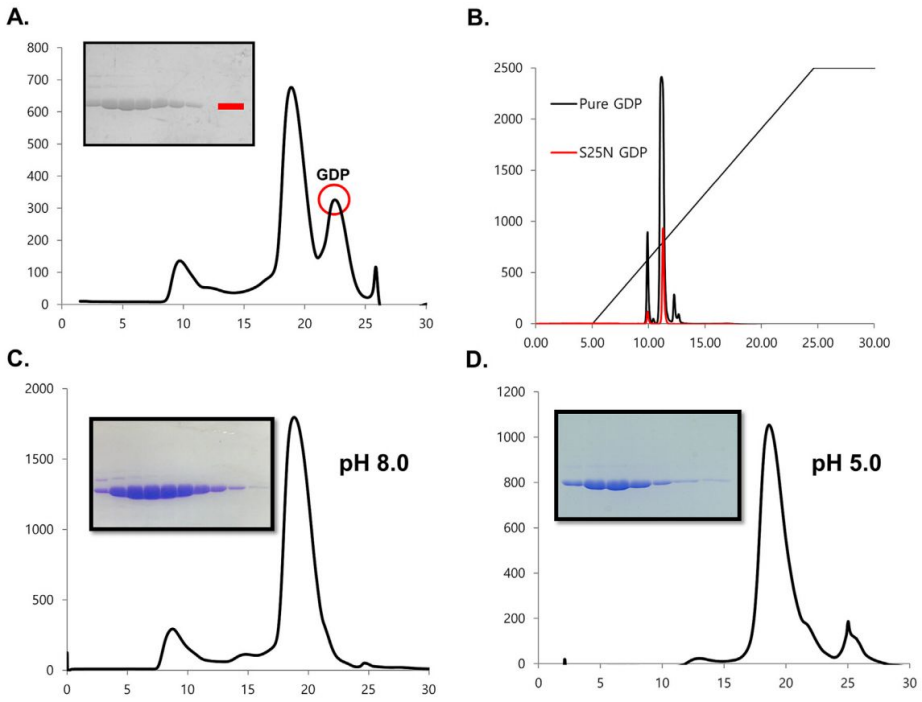

Figure 3. Gel filtration chromatogram and fractions of Rab11A S25N with GDP.

(A) The eluted Rab11A S25N with 200 μM of GDP applied onto a Superdex-200 gel filtration column (GE Healthcare) that had been pre-equilibrated with 20 mM Tris pH 8.0, 150 mM NaCl. Inset, an SDS-PAGE of the fractions from the peak of Rab11A S25N is shown. Red bar indicates the fractions where the peaks of GDP were detected (red circle). (B) Comparison of electric conductance value of GDP and boiled extract of Rab11A S25N. Mono Q column (GE Healthcare) was used for anion exchange chromatographic analysis. Rab11A S25N was purified using

GDP-containing elution buffer and then boiled under 373 K for 10 min. Denatured fragments were removed by centrifugation and the result was shown red. 1 mM of pure GDP was used for comparison control. (C-D) Size-exclusion chromatography was performed for purification of Rab11A S25N. The eluted Rab11A S25N with 200 μM of GDP applied onto a Superdex-200 gel filtration column that had been pre-equilibrated with 20 mM Tris pH 8.0, 150 mM NaCl, 50 μM GDP (C) and with 20 mM sodium citrate at pH 5.0, 150 mM NaCl and 50 μM GDP (D).

DISCUSSION

GTPase proteins function as molecular switches cycling the GTP-bound state (active state or 'ON'-state) and GDP-bound state (inactive state or 'OFF'-state). In the general GTPase cycle, the active state of GTPase is completed after both binding of GTP and coordination of Mg^{2+}. Once GTP binds to GTPase, coordination of Mg^{2+} induces closing of switch I, leading to hydrolysis to GDP by switch II. During this timing process, Mg^{2+} is located between the beta- and gamma-phosphate group of GTP and switch I of GTPase (Fig. 4A). If this composition is changed, for example, if GTP is hydrolyzed to GDP, Mg^{2+} is released, resulting in the release of GDP from GTPase or exchange to GTP. The rate of release step is protein type-dependent, but this is facilitated by guanine nucleotide exchange factors (GEFs). On the other hand, coordination of nucleotides in vitro depends on the affinity and concentration of guanine nucleotide and Mg^{2+} ion.

GDP-bound mutant was previously reported to perturb binding of Mg^{2+} to GTPase [150, 151]. Since the absence of Mg^{2+} in GTPase leads to reduced affinity for GTP, resulting in a GDP-bound state, GDP-bound mutant does not indicate a high

affinity for GDP. Therefore, if the GDP-bound mutant is purified under in vitro conditions without effector proteins, the nucleotide free-state or GDP-bound state depends only on affinity for GDP.

In my observations, Rab11A S25N had low stability. I thought the mutated residue might lead to a high tendency to release GDP from the nucleotide binding pocket, resulting in unstable protein. Molecular modeling indicated low affinity for GDP (Fig. 4B). S25 can coordinate with Mg^{2+}, which can coordinate with GTP; however, N25 cannot coordinate with Mg^{2+} or GDP in the nucleotide binding pocket (Fig. 4B). As previously reported and consistent with my results, the absence of GDP decreased the solubility and stability in the inactive mutant of the GTPase [153]. Arf6 T27N, which is an inactive mutant of Arf6 GTPase, was able to exist in cells via formation of complex with its exchange factor, and had a low affinity for nucleotides and low stability without GDP under in vitro conditions [153]. However, it is not always true that the inactive mutant form of GTPase does not have a sufficient affinity for GDP to exist as a GDP bound form under in vitro conditions. Rab1 S25N, which is the inactive mutant form of Rab1 GTPase, was crystallized without

the addition of GDP during the purification process, while the GDP in Rab1 S25N was well resolved with good electron density [154]. Taken together, the stability and affinity for GDP in GTPase is protein-type dependent.

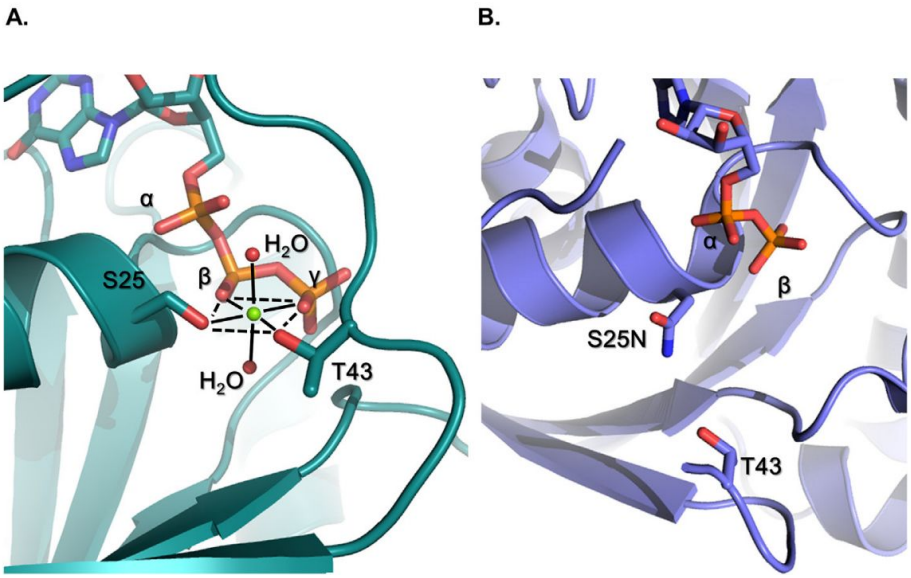

Figure 4. Homology modeling of Rab11A.

(A) Mg^{2+} coordination in wild type of Rab11A. Mg^{2+} associates with beta- and gamma-phosphate of GTP and serine at position 25. Association of switch I with Mg^{2+} through threonine at position 43 makes closed-form of Rab11A. (B) Prediction model of GDP binding pocket in Rab11A S25N. Overall structural model was rendered based on the X-ray structure of human Rab11A (PDB ID: 2F9L). Among possible directions of altered amino acid residue, I selected this direction based on other GDP bound form of Rab protein (PDB ID: 3SFV).

In the case of Rab11A, wild type and other mutants (S20V and Q70L) became highly soluble proteins with proper coordination of nucleotides. My experiments showed that loss of nucleotide was not detectable during the purification process (Fig. 1C). Recently, mygroup solved the three-dimensional structure of Rab11A S20V and Rab11A wild type and found that those proteins contained GTP at the nucleotide binding sites. Taken together, these findings strongly indicate that the solubility and stability of Rab11A is dependent on the proper binding of nucleotides in the binding pocket, and that the high stability by occupation of proper nucleotides in GTPase led to successful purification, crystallization and structure determination.

It is well known that the solubility and stability of a protein is proportional to the purity. Protein purity is one of the most important factors for crystallization during structural studies. Indeed, high purity of individual proteins provides advantages in biochemical experiments such as enabling enzyme activity analysis and identification of binding partners or validation of binding regions in partner proteins. Therefore, I extended my efforts to identify strategies to improve the stability of proteins such as changing the pH, temperature or region of the target

gene. Here, I demonstrated that Rab11A S25N was purified with high purity and stability by saturating GDP binding to Rab11A S25N. During this purification process, high stability of Rab11A S25N was maintained at all time by maintaining a suitable GDP concentration without changing any parameters such as buffer condition, temperature or plasmid construct. Using my method, I were finally able to purify approximately 20 mg/5-6 g of wet weight cells, which is comparable to the yield of the wild-type in the absence of GDP. My studies will provide a valuable guide for investigation of other small GTPase proteins.

CONCLUSION

Here, I solved crystal structures of Rab6A′ and active form of Rab11A. I report the crystal structure of the mutant form of human Rab6A′ (Q72L), which has been shown to be in a GTP lock form, at 1.9 Å resolution. Despite of low intrinsic activity, crystal structure of Rab6A′ was solved GDP bound form. In addition, switch I lost its stability which is commonly observed in GDP bound form. It is thought that the conformational rearrangement of switch II domain was triggered during crystallization, and Gln−22 alternatively activated water molecule for GTP hydrolysis. Interestingly, inactive form of Rab6A′ showed similar conformation to active form of Rab6A in several domain. Rab6A and Rab6A′ partly share cellular localization, pathway and binding partner. However specific role of them are slightly different. It is believed that this protein plays unique roles in several cellular processes due to different amino acid composition on binding interface which is opposite side of catalytic domain.

It has been reported that Rab11A functionally associates with Rab6A in several cellular processes and diseases, described above. The evidence of association with them is that they share

similar conformation despite they perform different role in cellular pathways. However, active form of Rab11A has not been determined. I solved Rab11A S20V, which is constitutively active form of Rab11A, and I determined how this protein could trap GTP. In addition, active Rab11A could share binding partner with Rab6A by comparison of structure between them.

Next, I analyzed protein stability of inactive form of Rab11A (S25N), it need occupation of GDP in vitro environment. Although I failed to crystallize it, stable purification of inactive form provides useful to understand biochemical property of Rab11A.

The information of Rab GTPase function in membrane trafficking and diseases has been increased. Despite the understanding of their role and effector protein in pathological mechanism, no therapeutic intervention has been still proposed. The best strategy to therapeutic approaches might be know the overall network rather than look at a single Rab member in isolation. However, we are beginning to understand how Rab GTPases communicate with each other. This communication depends on associated regulator protein and effector protein. In this issue, finding binding partner and analysis of consequential

function are needed to *in vitro* experiment. In addition, specific state of Rab GTPase should be used as bait for catching the partner. Furthermore, animal experiment is also required for investigating phenotype in disease model. Without utilizing of proper construct and understanding of enzymatic activity, it is hardly to find link of Rab GTPase to disease. My studies did not analyze the physiological role in the respective function and diseases between Rab11A and Rab6A. However, structural study of Rab11A and Rab6A open up the opportunity for gaining more insights into the role in Rab-related network and disease

REFERENCES

1. Matozaki, T., Nakanishi, H., and Takai, Y. (2000). Small G-protein networks: their crosstalk and signal cascades. Cell Signal *12*, 515-524.
2. Rossman, K.L., and Der, C.J. (2005). The Ras superfamily at a glance. Journal of Cell Science *118*, 4p.
3. Takai, Y., Kaibuchi, K., Kikuchi, A., and Kawata, M. (1992). Small GTP-binding proteins. Int Rev Cytol *133*, 187-230.
4. Vetter, I.R., and Wittinghofer, A. (2001). The guanine nucleotide-binding switch in three dimensions. Science *294*, 1299-1304.
5. Takai, Y., Sasaki, T., and Matozaki, T. (2001). Small GTP-binding proteins. Physiol Rev *81*, 153-208.
6. Bourne, H.R., Sanders, D.A., and McCormick, F. (1990). The GTPase superfamily: a conserved switch for diverse cell functions. Nature *348*, 125-132.
7. Hall, A. (1990). The cellular functions of small GTP-binding proteins. Science *249*, 635-640.
8. Ligeti, E., Welti, S., and Scheffzek, K. (2012). Inhibition and termination of physiological responses by GTPase activating proteins. Physiol Rev *92*, 237-272.
9. Simon, I., Zerial, M., and Goody, R.S. (1996). Kinetics of interaction of Rab5 and Rab7 with nucleotides and magnesium ions. J Biol Chem *271*, 20470-20478.
10. Itzen, A., and Goody, R.S. (2011). GTPases involved in vesicular trafficking: structures and mechanisms. Semin Cell Dev Biol *22*, 48-56.
11. Loirand, G., Sauzeau, V., and Pacaud, P. (2013). Small G proteins in the cardiovascular system: physiological and pathological aspects. Physiol Rev *93*, 1659-1720.
12. Macara, I.G., Lounsbury, K.M., Richards, S.A., McKiernan, C., and Bar-Sagi, D. (1996). The Ras superfamily of GTPases. FASEB J *10*, 625-630.
13. Grosshans, B.L., Ortiz, D., and Novick, P. (2006). Rabs and their effectors: achieving specificity in membrane traffic. Proc Natl Acad Sci U S A *103*, 11821-11827.
14. Andres, D.A., Seabra, M.C., Brown, M.S., Armstrong, S.A., Smeland, T.E., Cremers, F.P., and Goldstein, J.L. (1993). cDNA cloning of component A of Rab geranylgeranyl transferase and demonstration of its role as a Rab escort protein. Cell *73*, 1091-1099.
15. Hutagalung, A.H., and Novick, P.J. (2011). Role of Rab GTPases in membrane traffic and cell physiology. Physiol Rev *91*, 119-149.

16. Alexandrov, K., Horiuchi, H., Steele-Mortimer, O., Seabra, M.C., and Zerial, M. (1994). Rab escort protein-1 is a multifunctional protein that accompanies newly prenylated rab proteins to their target membranes. EMBO J *13*, 5262-5273.
17. Corbeel, L., and Freson, K. (2008). Rab proteins and Rab-associated proteins: major actors in the mechanism of protein-trafficking disorders. Eur J Pediatr *167*, 723-729.
18. Schimmoller, F., Simon, I., and Pfeffer, S.R. (1998). Rab GTPases, directors of vesicle docking. J Biol Chem *273*, 22161-22164.
19. Miserey-Lenkei, S., Waharte, F., Boulet, A., Cuif, M.H., Tenza, D., El Marjou, A., Raposo, G., Salamero, J., Heliot, L., Goud, B., et al. (2007). Rab6-interacting protein 1 links Rab6 and Rab11 function. Traffic *8*, 1385-1403.
20. Saito-Nakano, Y., Nakahara, T., Nakano, K., Nozaki, T., and Numata, O. (2010). Marked amplification and diversification of products of ras genes from rat brain, Rab GTPases, in the ciliates Tetrahymena thermophila and Paramecium tetraurelia. J Eukaryot Microbiol *57*, 389-399.
21. Lal, K., Field, M.C., Carlton, J.M., Warwicker, J., and Hirt, R.P. (2005). Identification of a very large Rab GTPase family in the parasitic protozoan Trichomonas vaginalis. Mol Biochem Parasitol *143*, 226-235.
22. Bock, J.B., Matern, H.T., Peden, A.A., and Scheller, R.H. (2001). A genomic perspective on membrane compartment organization. Nature *409*, 839-841.
23. Yoshimura, S., Gerondopoulos, A., Linford, A., Rigden, D.J., and Barr, F.A. (2010). Family-wide characterization of the DENN domain Rab GDP-GTP exchange factors. J Cell Biol *191*, 367-381.
24. Marat, A.L., Dokainish, H., and McPherson, P.S. (2011). DENN domain proteins: regulators of Rab GTPases. J Biol Chem *286*, 13791-13800.
25. Lachance, V., Cartier, A., Genier, S., Munger, S., Germain, P., Labrecque, P., and Parent, J.L. (2011). Regulation of beta2-adrenergic receptor maturation and anterograde trafficking by an interaction with Rab geranylgeranyltransferase: modulation of Rab geranylgeranylation by the receptor. J Biol Chem *286*, 40802-40813.
26. Segev, N. (2001). Ypt/rab gtpases: regulators of protein trafficking. Sci STKE *2001*, re11.
27. Pfeffer, S.R. (2001). Rab GTPases: specifying and deciphering organelle identity and function. Trends Cell Biol *11*, 487-491.
28. Sivars, U., Aivazian, D., and Pfeffer, S.R. (2003). Yip3 catalyses the dissociation of endosomal Rab-GDI complexes. Nature *425*, 856-859.

29. Collins, R.N. (2003). "Getting it on"--GDI displacement and small GTPase membrane recruitment. Mol Cell *12*, 1064-1066.
30. Goud, B., Zahraoui, A., Tavitian, A., and Saraste, J. (1990). Small GTP-binding protein associated with Golgi cisternae. Nature *345*, 553-556.
31. Martinez, O., Schmidt, A., Salamero, J., Hoflack, B., Roa, M., and Goud, B. (1994). The small GTP-binding protein rab6 functions in intra-Golgi transport. J Cell Biol *127*, 1575-1588.
32. Chavrier, P., Parton, R.G., Hauri, H.P., Simons, K., and Zerial, M. (1990). Localization of low molecular weight GTP binding proteins to exocytic and endocytic compartments. Cell *62*, 317-329.
33. Antony, C., Cibert, C., Geraud, G., Santa Maria, A., Maro, B., Mayau, V., and Goud, B. (1992). The small GTP-binding protein rab6p is distributed from medial Golgi to the trans-Golgi network as determined by a confocal microscopic approach. J Cell Sci *103 (Pt 3)*, 785-796.
34. D'Adamo, P., Menegon, A., Lo Nigro, C., Grasso, M., Gulisano, M., Tamanini, F., Bienvenu, T., Gedeon, A.K., Oostra, B., Wu, S.K., et al. (1998). Mutations in GDI1 are responsible for X-linked non-specific mental retardation. Nat Genet *19*, 134-139.
35. Leaf, D.S., and Blum, L.D. (1998). Analysis of rab10 localization in sea urchin embryonic cells by three-dimensional reconstruction. Exp Cell Res *243*, 39-49.
36. Babbey, C.M., Ahktar, N., Wang, E., Chen, C.C., Grant, B.D., and Dunn, K.W. (2006). Rab10 regulates membrane transport through early endosomes of polarized Madin-Darby canine kidney cells. Mol Biol Cell *17*, 3156-3175.
37. Junutula, J.R., De Maziere, A.M., Peden, A.A., Ervin, K.E., Advani, R.J., van Dijk, S.M., Klumperman, J., and Scheller, R.H. (2004). Rab14 is involved in membrane trafficking between the Golgi complex and endosomes. Mol Biol Cell *15*, 2218-2229.
38. Larance, M., Ramm, G., Stockli, J., van Dam, E.M., Winata, S., Wasinger, V., Simpson, F., Graham, M., Junutula, J.R., Guilhaus, M., et al. (2005). Characterization of the role of the Rab GTPase-activating protein AS160 in insulin-regulated GLUT4 trafficking. J Biol Chem *280*, 37803-37813.
39. Chen, S., Liang, M.C., Chia, J.N., Ngsee, J.K., and Ting, A.E. (2001). Rab8b and its interacting partner TRIP8b are involved in regulated secretion in AtT20 cells. J Biol Chem *276*, 13209-13216.
40. Fukuda, M. (2003). Distinct Rab binding specificity of Rim1, Rim2, rabphilin, and Noc2. Identification of a critical determinant of Rab3A/Rab27A recognition by Rim2. J Biol Chem *278*, 15373-15380.
41. Cortes, C., Rzomp, K.A., Tvinnereim, A., Scidmore, M.A., and

Wizel, B. (2007). Chlamydia pneumoniae inclusion membrane protein Cpn0585 interacts with multiple Rab GTPases. Infect Immun *75*, 5586-5596.
42. Fukuda, M., Kanno, E., Ishibashi, K., and Itoh, T. (2008). Large scale screening for novel rab effectors reveals unexpected broad Rab binding specificity. Mol Cell Proteomics *7*, 1031-1042.
43. Kelly, E.E., Horgan, C.P., Adams, C., Patzer, T.M., Ni Shuilleabhain, D.M., Norman, J.C., and McCaffrey, M.W. (2010). Class I Rab11-family interacting proteins are binding targets for the Rab14 GTPase. Biol Cell *102*, 51-62.
44. Fischer von Mollard, G., Mignery, G.A., Baumert, M., Perin, M.S., Hanson, T.J., Burger, P.M., Jahn, R., and Sudhof, T.C. (1990). rab3 is a small GTP-binding protein exclusively localized to synaptic vesicles. Proc Natl Acad Sci U S A *87*, 1988-1992.
45. Masuda, E.S., Luo, Y., Young, C., Shen, M., Rossi, A.B., Huang, B.C., Yu, S., Bennett, M.K., Payan, D.G., and Scheller, R.H. (2000). Rab37 is a novel mast cell specific GTPase localized to secretory granules. FEBS Lett *470*, 61-64.
46. Yoshie, S., Imai, A., Nashida, T., and Shimomura, H. (2000). Expression, characterization, and localization of Rab26, a low molecular weight GTP-binding protein, in the rat parotid gland. Histochem Cell Biol *113*, 259-263.
47. Hume, A.N., Collinson, L.M., Rapak, A., Gomes, A.Q., Hopkins, C.R., and Seabra, M.C. (2001). Rab27a regulates the peripheral distribution of melanosomes in melanocytes. J Cell Biol *152*, 795-808.
48. Jager, D., Stockert, E., Jager, E., Gure, A.O., Scanlan, M.J., Knuth, A., Old, L.J., and Chen, Y.T. (2000). Serological cloning of a melanocyte rab guanosine 5'-triphosphate-binding protein and a chromosome condensation protein from a melanoma complementary DNA library. Cancer Res *60*, 3584-3591.
49. Alto, N.M., Soderling, J., and Scott, J.D. (2002). Rab32 is an A-kinase anchoring protein and participates in mitochondrial dynamics. J Cell Biol *158*, 659-668.
50. Tamura, K., Ohbayashi, N., Maruta, Y., Kanno, E., Itoh, T., and Fukuda, M. (2009). Varp is a novel Rab32/38-binding protein that regulates Tyrp1 trafficking in melanocytes. Mol Biol Cell *20*, 2900-2908.
51. Christoforidis, S., McBride, H.M., Burgoyne, R.D., and Zerial, M. (1999). The Rab5 effector EEA1 is a core component of endosome docking. Nature *397*, 621-625.
52. Callaghan, J., Nixon, S., Bucci, C., Toh, B.H., and Stenmark, H. (1999). Direct interaction of EEA1 with Rab5b. Eur J Biochem *265*, 361-366.
53. Christoforidis, S., Miaczynska, M., Ashman, K., Wilm, M., Zhao,

L., Yip, S.C., Waterfield, M.D., Backer, J.M., and Zerial, M. (1999). Phosphatidylinositol-3-OH kinases are Rab5 effectors. Nat Cell Biol *1*, 249-252.

54. Cantalupo, G., Alifano, P., Roberti, V., Bruni, C.B., and Bucci, C. (2001). Rab-interacting lysosomal protein (RILP): the Rab7 effector required for transport to lysosomes. EMBO J *20*, 683-693.
55. Zuk, P.A., and Elferink, L.A. (1999). Rab15 mediates an early endocytic event in Chinese hamster ovary cells. J Biol Chem *274*, 22303-22312.
56. van der Sluijs, P., Hull, M., Webster, P., Male, P., Goud, B., and Mellman, I. (1992). The small GTP-binding protein rab4 controls an early sorting event on the endocytic pathway. Cell *70*, 729-740.
57. Urbe, S., Huber, L.A., Zerial, M., Tooze, S.A., and Parton, R.G. (1993). Rab11, a small GTPase associated with both constitutive and regulated secretory pathways in PC12 cells. FEBS Lett *334*, 175-182.
58. Lindsay, A.J., Hendrick, A.G., Cantalupo, G., Senic-Matuglia, F., Goud, B., Bucci, C., and McCaffrey, M.W. (2002). Rab coupling protein (RCP), a novel Rab4 and Rab11 effector protein. J Biol Chem *277*, 12190-12199.
59. Ozeki, S., Cheng, J., Tauchi-Sato, K., Hatano, N., Taniguchi, H., and Fujimoto, T. (2005). Rab18 localizes to lipid droplets and induces their close apposition to the endoplasmic reticulum-derived membrane. J Cell Sci *118*, 2601-2611.
60. Olkkonen, V.M., Dupree, P., Killisch, I., Lutcke, A., Zerial, M., and Simons, K. (1993). Molecular cloning and subcellular localization of three GTP-binding proteins of the rab subfamily. J Cell Sci *106 (Pt 4)*, 1249-1261.
61. Zheng, J.Y., Koda, T., Fujiwara, T., Kishi, M., Ikehara, Y., and Kakinuma, M. (1998). A novel Rab GTPase, Rab33B, is ubiquitously expressed and localized to the medial Golgi cisternae. J Cell Sci *111 (Pt 8)*, 1061-1069.
62. Valsdottir, R., Hashimoto, H., Ashman, K., Koda, T., Storrie, B., and Nilsson, T. (2001). Identification of rabaptin-5, rabex-5, and GM130 as putative effectors of rab33b, a regulator of retrograde traffic between the Golgi apparatus and ER. FEBS Lett *508*, 201-209.
63. Nakamura, S., Takemura, T., Tan, L., Nagata, Y., Yokota, D., Hirano, I., Shigeno, K., Shibata, K., Fujie, M., Fujisawa, S., et al. (2011). Small GTPase RAB45-mediated p38 activation in apoptosis of chronic myeloid leukemia progenitor cells. Carcinogenesis *32*, 1758-1772.
64. Casanova, J.E., Wang, X., Kumar, R., Bhartur, S.G., Navarre, J., Woodrum, J.E., Altschuler, Y., Ray, G.S., and Goldenring, J.R.

(1999). Association of Rab25 and Rab11a with the apical recycling system of polarized Madin-Darby canine kidney cells. Mol Biol Cell *10*, 47-61.

65. Simpson, J.C., Griffiths, G., Wessling-Resnick, M., Fransen, J.A., Bennett, H., and Jones, A.T. (2004). A role for the small GTPase Rab21 in the early endocytic pathway. J Cell Sci *117*, 6297-6311.
66. Pellinen, T., Arjonen, A., Vuoriluoto, K., Kallio, K., Fransen, J.A., and Ivaska, J. (2006). Small GTPase Rab21 regulates cell adhesion and controls endosomal traffic of beta1-integrins. J Cell Biol *173*, 767-780.
67. Caswell, P.T., Spence, H.J., Parsons, M., White, D.P., Clark, K., Cheng, K.W., Mills, G.B., Humphries, M.J., Messent, A.J., Anderson, K.I., et al. (2007). Rab25 associates with alpha5beta1 integrin to promote invasive migration in 3D microenvironments. Dev Cell *13*, 496-510.
68. Zahraoui, A., Joberty, G., Arpin, M., Fontaine, J.J., Hellio, R., Tavitian, A., and Louvard, D. (1994). A small rab GTPase is distributed in cytoplasmic vesicles in non polarized cells but colocalizes with the tight junction marker ZO-1 in polarized epithelial cells. J Cell Biol *124*, 101-115.
69. Lutcke, A., Jansson, S., Parton, R.G., Chavrier, P., Valencia, A., Huber, L.A., Lehtonen, E., and Zerial, M. (1993). Rab17, a novel small GTPase, is specific for epithelial cells and is induced during cell polarization. J Cell Biol *121*, 553-564.
70. Hunziker, W., and Peters, P.J. (1998). Rab17 localizes to recycling endosomes and regulates receptor-mediated transcytosis in epithelial cells. J Biol Chem *273*, 15734-15741.
71. Lutcke, A., Olkkonen, V.M., Dupree, P., Lutcke, H., Simons, K., and Zerial, M. (1995). Isolation of a murine cDNA clone encoding Rab19, a novel tissue-specific small GTPase. Gene *155*, 257-260.
72. de Leeuw, H.P., Koster, P.M., Calafat, J., Janssen, H., van Zonneveld, A.J., van Mourik, J.A., and Voorberg, J. (1998). Small GTP-binding proteins in human endothelial cells. Br J Haematol *103*, 15-19.
73. Chen, T., Han, Y., Yang, M., Zhang, W., Li, N., Wan, T., Guo, J., and Cao, X. (2003). Rab39, a novel Golgi-associated Rab GTPase from human dendritic cells involved in cellular endocytosis. Biochem Biophys Res Commun *303*, 1114-1120.
74. Haas, A.K., Fuchs, E., Kopajtich, R., and Barr, F.A. (2005). A GTPase-activating protein controls Rab5 function in endocytic trafficking. Nat Cell Biol *7*, 887-893.
75. Chen, L., Hu, J., Yun, Y., and Wang, T. (2010). Rab36 regulates the spatial distribution of late endosomes and lysosomes through a similar mechanism to Rab34. Mol Membr Biol *27*, 23-

30.
76. Rhodes, D.R., Kalyana-Sundaram, S., Mahavisno, V., Varambally, R., Yu, J., Briggs, B.B., Barrette, T.R., Anstet, M.J., Kincead-Beal, C., Kulkarni, P., et al. (2007). Oncomine 3.0: genes, pathways, and networks in a collection of 18,000 cancer gene expression profiles. Neoplasia *9*, 166-180.
77. Culine, S., Honore, N., Closson, V., Droz, J.P., Extra, J.M., Marty, M., Tavitian, A., and Olofsson, B. (1994). A small GTP-binding protein is frequently overexpressed in peripheral blood mononuclear cells from patients with solid tumours. Eur J Cancer *30A*, 670-674.
78. Verhoeven, K., De Jonghe, P., Coen, K., Verpoorten, N., Auer-Grumbach, M., Kwon, J.M., FitzPatrick, D., Schmedding, E., De Vriendt, E., Jacobs, A., et al. (2003). Mutations in the small GTP-ase late endosomal protein RAB7 cause Charcot-Marie-Tooth type 2B neuropathy. Am J Hum Genet *72*, 722-727.
79. Amillet, J.M., Ferbus, D., Real, F.X., Antony, C., Muleris, M., Gress, T.M., and Goubin, G. (2006). Characterization of human Rab20 overexpressed in exocrine pancreatic carcinoma. Hum Pathol *37*, 256-263.
80. Kotzsch, M., Sieuwerts, A.M., Grosser, M., Meye, A., Fuessel, S., Meijer-van Gelder, M.E., Smid, M., Schmitt, M., Baretton, G., Luther, T., et al. (2008). Urokinase receptor splice variant uPAR-del4/5-associated gene expression in breast cancer: identification of rab31 as an independent prognostic factor. Breast Cancer Res Treat *111*, 229-240.
81. Tan, P.Y., Chang, C.W., Chng, K.R., Wansa, K.D., Sung, W.K., and Cheung, E. (2012). Integration of regulatory networks by NKX3-1 promotes androgen-dependent prostate cancer survival. Mol Cell Biol *32*, 399-414.
82. He, H., Dai, F., Yu, L., She, X., Zhao, Y., Jiang, J., Chen, X., and Zhao, S. (2002). Identification and characterization of nine novel human small GTPases showing variable expressions in liver cancer tissues. Gene Expr *10*, 231-242.
83. Mor, O., Nativ, O., Stein, A., Novak, L., Lehavi, D., Shiboleth, Y., Rozen, A., Berent, E., Brodsky, L., Feinstein, E., et al. (2003). Molecular analysis of transitional cell carcinoma using cDNA microarray. Oncogene *22*, 7702-7710.
84. Korkola, J.E., Heck, S., Olshen, A.B., Reuter, V.E., Bosl, G.J., Houldsworth, J., and Chaganti, R.S. (2008). In vivo differentiation and genomic evolution in adult male germ cell tumors. Genes Chromosomes Cancer *47*, 43-55.
85. Agarwal, R., Jurisica, I., Mills, G.B., and Cheng, K.W. (2009). The emerging role of the RAB25 small GTPase in cancer. Traffic *10*, 1561-1568.
86. Rzomp, K.A., Scholtes, L.D., Briggs, B.J., Whittaker, G.R., and

Scidmore, M.A. (2003). Rab GTPases are recruited to chlamydial inclusions in both a species-dependent and species-independent manner. Infect Immun *71*, 5855-5870.
87. Nam, K.T., Lee, H.J., Smith, J.J., Lapierre, L.A., Kamath, V.P., Chen, X., Aronow, B.J., Yeatman, T.J., Bhartur, S.G., Calhoun, B.C., et al. (2010). Loss of Rab25 promotes the development of intestinal neoplasia in mice and is associated with human colorectal adenocarcinomas. J Clin Invest *120*, 840-849.
88. Fu, D., and Arias, I.M. (2012). Intracellular trafficking of P-glycoprotein. Int J Biochem Cell Biol *44*, 461-464.
89. Ferrandiz-Huertas, C., Fernandez-Carvajal, A., and Ferrer-Montiel, A. (2011). Rab4 interacts with the human P-glycoprotein and modulates its surface expression in multidrug resistant K562 cells. Int J Cancer *128*, 192-205.
90. Shan, J., Mason, J.M., Yuan, L., Barcia, M., Porti, D., Calabro, A., Budman, D., Vinciguerra, V., and Xu, H. (2000). Rab6c, a new member of the rab gene family, is involved in drug resistance in MCF7/AdrR cells. Gene *257*, 67-75.
91. Eggenschwiler, J.T., Espinoza, E., and Anderson, K.V. (2001). Rab23 is an essential negative regulator of the mouse Sonic hedgehog signalling pathway. Nature *412*, 194-198.
92. Scheper, W., Hoozemans, J.J., Hoogenraad, C.C., Rozemuller, A.J., Eikelenboom, P., and Baas, F. (2007). Rab6 is increased in Alzheimer's disease brain and correlates with endoplasmic reticulum stress. Neuropathol Appl Neurobiol *33*, 523-532.
93. Ginsberg, S.D., Alldred, M.J., Counts, S.E., Cataldo, A.M., Neve, R.L., Jiang, Y., Wuu, J., Chao, M.V., Mufson, E.J., Nixon, R.A., et al. (2010). Microarray analysis of hippocampal CA1 neurons implicates early endosomal dysfunction during Alzheimer's disease progression. Biol Psychiatry *68*, 885-893.
94. Moussaud, S., Jones, D.R., Moussaud-Lamodiere, E.L., Delenclos, M., Ross, O.A., and McLean, P.J. (2014). Alpha-synuclein and tau: teammates in neurodegeneration? Mol Neurodegener *9*, 43.
95. Bhuin, T., and Roy, J.K. (2015). Rab11 in disease progression. Int J Mol Cell Med *4*, 1-8.
96. Ullrich, O., Reinsch, S., Urbe, S., Zerial, M., and Parton, R.G. (1996). Rab11 regulates recycling through the pericentriolar recycling endosome. J Cell Biol *135*, 913-924.
97. Ren, M., Xu, G., Zeng, J., De Lemos-Chiarandini, C., Adesnik, M., and Sabatini, D.D. (1998). Hydrolysis of GTP on rab11 is required for the direct delivery of transferrin from the pericentriolar recycling compartment to the cell surface but not from sorting endosomes. Proc Natl Acad Sci U S A *95*, 6187-6192.
98. Cox, D., Lee, D.J., Dale, B.M., Calafat, J., and Greenberg, S.

(2000). A Rab11-containing rapidly recycling compartment in macrophages that promotes phagocytosis. Proc Natl Acad Sci U S A *97*, 680-685.

99. Elfrink, H.L., Zwart, R., Cavanillas, M.L., Schindler, A.J., Baas, F., and Scheper, W. (2012). Rab6 is a modulator of the unfolded protein response: implications for Alzheimer's disease. J Alzheimers Dis *28*, 917-929.
100. Ni, Y., Zhao, X., Bao, G., Zou, L., Teng, L., Wang, Z., Song, M., Xiong, J., Bai, Y., and Pei, G. (2006). Activation of beta2-adrenergic receptor stimulates gamma-secretase activity and accelerates amyloid plaque formation. Nat Med *12*, 1390-1396.
101. Ross, J.A., McGonigle, P., and Van Bockstaele, E.J. (2015). Locus Coeruleus, norepinephrine and Abeta peptides in Alzheimer's disease. Neurobiol Stress *2*, 73-84.
102. Rejman Lipinski, A., Heymann, J., Meissner, C., Karlas, A., Brinkmann, V., Meyer, T.F., and Heuer, D. (2009). Rab6 and Rab11 regulate Chlamydia trachomatis development and golgin-84-dependent Golgi fragmentation. PLoS Pathog *5*, e1000615.
103. Heuer, D., Rejman Lipinski, A., Machuy, N., Karlas, A., Wehrens, A., Siedler, F., Brinkmann, V., and Meyer, T.F. (2009). Chlamydia causes fragmentation of the Golgi compartment to ensure reproduction. Nature *457*, 731-735.
104. Hou, X., Hagemann, N., Schoebel, S., Blankenfeldt, W., Goody, R.S., Erdmann, K.S., and Itzen, A. (2011). A structural basis for Lowe syndrome caused by mutations in the Rab-binding domain of OCRL1. EMBO J *30*, 1659-1670.
105. van de Graaf, S.F., Chang, Q., Mensenkamp, A.R., Hoenderop, J.G., and Bindels, R.J. (2006). Direct interaction with Rab11a targets the epithelial Ca2+ channels TRPV5 and TRPV6 to the plasma membrane. Mol Cell Biol *26*, 303-312.
106. Wu, G., Zhang, W., Na, T., Jing, H., Wu, H., and Peng, J.B. (2012). Suppression of intestinal calcium entry channel TRPV6 by OCRL, a lipid phosphatase associated with Lowe syndrome and Dent disease. Am J Physiol Cell Physiol *302*, C1479-1491.
107. Wilson, G.M., Fielding, A.B., Simon, G.C., Yu, X., Andrews, P.D., Hames, R.S., Frey, A.M., Peden, A.A., Gould, G.W., and Prekeris, R. (2005). The FIP3-Rab11 protein complex regulates recycling endosome targeting to the cleavage furrow during late cytokinesis. Mol Biol Cell *16*, 849-860.
108. Miserey-Lenkei, S., Couedel-Courteille, A., Del Nery, E., Bardin, S., Piel, M., Racine, V., Sibarita, J.B., Perez, F., Bornens, M., and Goud, B. (2006). A role for the Rab6A' GTPase in the inactivation of the Mad2-spindle checkpoint. EMBO J *25*, 278-289.
109. Eggers, C.T., Schafer, J.C., Goldenring, J.R., and Taylor, S.S. (2009). D-AKAP2 interacts with Rab4 and Rab11 through its

RGS domains and regulates transferrin receptor recycling. J Biol Chem *284*, 32869-32880.
110. Bergbrede, T., Chuky, N., Schoebel, S., Blankenfeldt, W., Geyer, M., Fuchs, E., Goody, R.S., Barr, F., and Alexandrov, K. (2009). Biophysical analysis of the interaction of Rab6a GTPase with its effector domains. J Biol Chem *284*, 2628-2635.
111. Shin, Y.C., Seo, E.K., Jeon, J.H., and Park, H.H. (2013). Crystallization and preliminary X-ray crystallographic studies of the coiled-coil domain of PIST. Acta Crystallogr Sect F Struct Biol Cryst Commun *69*, 468-471.
112. Otwinowski, Z., and Minor, W. (1997). Processing of X-ray diffraction data collected in oscillation mode. Macromolecular Crystallography, Pt A *276*, 307-326.
113. Bergbrede, T., Pylypenko, O., Rak, A., and Alexandrov, K. (2005). Structure of the extremely slow GTPase Rab6A in the GTP bound form at 1.8A resolution. J Struct Biol *152*, 235-238.
114. Emsley, P., and Cowtan, K. (2004). Coot: model-building tools for molecular graphics. Acta Crystallogr D Biol Crystallogr *60*, 2126-2132.
115. Vagin, A.A., Steiner, R.A., Lebedev, A.A., Potterton, L., McNicholas, S., Long, F., and Murshudov, G.N. (2004). REFMAC5 dictionary: organization of prior chemical knowledge and guidelines for its use. Acta Crystallogr D Biol Crystallogr *60*, 2184-2195.
116. Echard, A., Opdam, F.J., de Leeuw, H.J., Jollivet, F., Savelkoul, P., Hendriks, W., Voorberg, J., Goud, B., and Fransen, J.A. (2000). Alternative splicing of the human Rab6A gene generates two close but functionally different isoforms. Mol Biol Cell *11*, 3819-3833.
117. Opdam, F.J., Echard, A., Croes, H.J., van den Hurk, J.A., van de Vorstenbosch, R.A., Ginsel, L.A., Goud, B., and Fransen, J.A. (2000). The small GTPase Rab6B, a novel Rab6 subfamily member, is cell-type specifically expressed and localised to the Golgi apparatus. J Cell Sci *113 (Pt 15)*, 2725-2735.
118. Fitzgerald, M.L., and Reed, G.L. (1999). Rab6 is phosphorylated in thrombin-activated platelets by a protein kinase C-dependent mechanism: effects on GTP/GDP binding and cellular distribution. Biochem J *342 (Pt 2)*, 353-360.
119. Echard, A., Jollivet, F., Martinez, O., Lacapere, J.J., Rousselet, A., Janoueix-Lerosey, I., and Goud, B. (1998). Interaction of a Golgi-associated kinesin-like protein with Rab6. Science *279*, 580-585.
120. Pai, E.F. (1998). The alpha and beta of turning on a molecular switch. Nat Struct Biol *5*, 259-263.
121. Yang, C., Mollat, P., Chaffotte, A., McCaffrey, M., Cabanie, L., and Goud, B. (1993). Comparison of the biochemical properties

of unprocessed and processed forms of the small GTP-binding protein, rab6p. Eur J Biochem *217*, 1027-1037.
122. Shimizu, T., Ihara, K., Maesaki, R., Kuroda, S., Kaibuchi, K., and Hakoshima, T. (2000). An open conformation of switch I revealed by the crystal structure of a Mg2+ -free form of RHOA complexed with GDP. Implications for the GDP/GTP exchange mechanism. J Biol Chem *275*, 18311-18317.
123. Holm, L., and Sander, C. (1995). Dali: a network tool for protein structure comparison. Trends Biochem Sci *20*, 478-480.
124. Chattopadhyay, D., Langsley, G., Carson, M., Recacha, R., DeLucas, L., and Smith, C. (2000). Structure of the nucleotide-binding domain of Plasmodium falciparum rab6 in the GDP-bound form. In Acta Crystallogr D Biol Crystallogr, Volume 56. pp. 937-944.
125. Garcia-Saez, I., Tcherniuk, S., and Kozielski, F. (2006). The structure of human neuronal Rab6B in the active and inactive form. Acta Crystallogr D Biol Crystallogr *62*, 725-733.
126. Eathiraj, S., Pan, X., Ritacco, C., and Lambright, D.G. (2005). Structural basis of family-wide Rab GTPase recognition by rabenosyn-5. Nature *436*, 415-419.
127. Stroupe, C., and Brunger, A.T. (2000). Crystal structures of a Rab protein in its inactive and active conformations. J Mol Biol *304*, 585-598.
128. Janoueix-Lerosey, I., Jollivet, F., Camonis, J., Marche, P.N., and Goud, B. (1995). Two-hybrid system screen with the small GTP-binding protein Rab6. Identification of a novel mouse GDP dissociation inhibitor isoform and two other potential partners of Rab6. J Biol Chem *270*, 14801-14808.
129. Kim, C.M., Choi, J.Y., Yoon, J.H., and Park, H.H. (2015). Purification, crystallization and X-ray crystallographic analysis of human RAB11(S20V), a constitutively active GTP-binding form. Acta Crystallogr F Struct Biol Commun *71*, 1247-1250.
130. McCoy, A.J., Grosse-Kunstleve, R.W., Adams, P.D., Winn, M.D., Storoni, L.C., and Read, R.J. (2007). Phaser crystallographic software. J Appl Crystallogr *40*, 658-674.
131. Pasqualato, S., Senic-Matuglia, F., Renault, L., Goud, B., Salamero, J., and Cherfils, J. (2004). The structural GDP/GTP cycle of Rab11 reveals a novel interface involved in the dynamics of recycling endosomes. J Biol Chem *279*, 11480-11488.
132. Laskowski, R.A., MacArthur, M.W., Moss, D.S., and Thornton, J.M. (1993). PROCHECK: a program to check the stereochemical quality of protein structures. Journal of Applied Crystallography *26*, 283-291.
133. Wang, X., Kumar, R., Navarre, J., Casanova, J.E., and Goldenring, J.R. (2000). Regulation of vesicle trafficking in madin-darby

canine kidney cells by Rab11a and Rab25. J Biol Chem *275*, 29138-29146.
134. Shin, Y.C., Yoon, J.H., Jang, T.H., Kim, S.Y., Heo, W.D., So, I., Jeon, J.H., and Park, H.H. (2012). Crystal structure of Rab6A'(Q72L) mutant reveals unexpected GDP/Mg(2)(+) binding with opened GTP-binding domain. Biochem Biophys Res Commun *424*, 269-273.
135. Pasqualato, S., and Cherfils, J. (2005). Crystallographic evidence for substrate-assisted GTP hydrolysis by a small GTP binding protein. Structure *13*, 533-540.
136. Scapin, S.M., Carneiro, F.R., Alves, A.C., Medrano, F.J., Guimaraes, B.G., and Zanchin, N.I. (2006). The crystal structure of the small GTPase Rab11b reveals critical differences relative to the Rab11a isoform. J Struct Biol *154*, 260-268.
137. Muller, M.P., Peters, H., Blumer, J., Blankenfeldt, W., Goody, R.S., and Itzen, A. (2010). The Legionella effector protein DrrA AMPylates the membrane traffic regulator Rab1b. Science *329*, 946-949.
138. Mishra, A.K., Del Campo, C.M., Collins, R.E., Roy, C.R., and Lambright, D.G. (2013). The Legionella pneumophila GTPase activating protein LepB accelerates Rab1 deactivation by a non-canonical hydrolytic mechanism. J Biol Chem *288*, 24000-24011.
139. Pai, E.F., Krengel, U., Petsko, G.A., Goody, R.S., Kabsch, W., and Wittinghofer, A. (1990). Refined crystal structure of the triphosphate conformation of H-ras p21 at 1.35 A resolution: implications for the mechanism of GTP hydrolysis. EMBO J *9*, 2351-2359.
140. Muraoka, S., Shima, F., Araki, M., Inoue, T., Yoshimoto, A., Ijiri, Y., Seki, N., Tamura, A., Kumasaka, T., Yamamoto, M., et al. (2012). Crystal structures of the state 1 conformations of the GTP-bound H-Ras protein and its oncogenic G12V and Q61L mutants. FEBS Lett *586*, 1715-1718.
141. Krengel, U., Schlichting, I., Scherer, A., Schumann, R., Frech, M., John, J., Kabsch, W., Pai, E.F., and Wittinghofer, A. (1990). Three-dimensional structures of H-ras p21 mutants: molecular basis for their inability to function as signal switch molecules. Cell *62*, 539-548.
142. Saraste, M., Sibbald, P.R., and Wittinghofer, A. (1990). The P-loop--a common motif in ATP- and GTP-binding proteins. Trends Biochem Sci *15*, 430-434.
143. Bunney, T.D., Opaleye, O., Roe, S.M., Vatter, P., Baxendale, R.W., Walliser, C., Everett, K.L., Josephs, M.B., Christow, C., Rodrigues-Lima, F., et al. (2009). Structural insights into formation of an active signaling complex between Rac and phospholipase C gamma 2. Mol Cell *34*, 223-233.
144. Rinaldi, F.C., Packer, M., and Collins, R. (2015). New insights

into the molecular mechanism of the Rab GTPase Sec4p activation. BMC Struct Biol *15*, 14.
145. Bondos, S.E., and Bicknell, A. (2003). Detection and prevention of protein aggregation before, during, and after purification. Anal Biochem *316*, 223-231.
146. Eathiraj, S., Mishra, A., Prekeris, R., and Lambright, D.G. (2006). Structural basis for Rab11-mediated recruitment of FIP3 to recycling endosomes. J Mol Biol *364*, 121-135.
147. Chen, W., Feng, Y., Chen, D., and Wandinger-Ness, A. (1998). Rab11 is required for trans-golgi network-to-plasma membrane transport and a preferential target for GDP dissociation inhibitor. Mol Biol Cell *9*, 3241-3257.
148. Mori, K., Hata, M., Neya, S., and Hoshino, T. (2005). Common semiopen conformations of Mg2+ -free Ras, Rho, Rab, Arf, and Ran proteins combined with GDP and their similarity with GEF-bound forms. J Am Chem Soc *127*, 15127-15137.
149. Shutes, A., Phillips, R.A., Corrie, J.E., and Webb, M.R. (2002). Role of magnesium in nucleotide exchange on the small G protein rac investigated using novel fluorescent Guanine nucleotide analogues. Biochemistry *41*, 3828-3835.
150. Pan, J.Y., Sanford, J.C., and Wessling-Resnick, M. (1996). Influence of Mg2+ on the structure and function of Rab5. J Biol Chem *271*, 1322-1328.
151. Nuoffer, C., Davidson, H.W., Matteson, J., Meinkoth, J., and Balch, W.E. (1994). A GDP-bound of rab1 inhibits protein export from the endoplasmic reticulum and transport between Golgi compartments. J Cell Biol *125*, 225-237.
152. Kremmer, T., Paulik, E., Boldizsar, M., and Holenyi, I. (1989). Application of the fast protein liquid chromatographic system and MonoQ HR 5/5 anion exchanger to the separation of nucleotides. J Chromatogr *493*, 45-52.
153. Macia, E., Luton, F., Partisani, M., Cherfils, J., Chardin, P., and Franco, M. (2004). The GDP-bound form of Arf6 is located at the plasma membrane. J Cell Sci *117*, 2389-2398.
154. Cheng, W., Yin, K., Lu, D., Li, B., Zhu, D., Chen, Y., Zhang, H., Xu, S., Chai, J., and Gu, L. (2012). Structural insights into a unique Legionella pneumophila effector LidA recognizing both GDP and GTP bound Rab1 in their active state. PLoS Pathog *8*, e1002528.

국문 초록

Ras 과의 구아노신삼인산-가수분해효소는 여러 세포과정들에서 중요한 역할을 수행한다. 구아노신삼인산-가수분해효소들은 구아노신삼인산이나 구아노신이인산의 결합 상태에 따라 효소의 활성이 조절된다. 구아노신삼인산이 이 효소에 결합하였을때는 활성 형태가 되며, 활성 형태의 효소는 구아노신삼인산을 구아노신이인산과 인산기로 분해한 뒤 비활성 형태로 바뀐다. Ras 과의 구아노신삼인산-가수분해효소 중 Rab 구아노신삼인산 가수분해효소는 내포작용과 생합성, 세포분화 및 세포성장 과정에서 일어나는 소낭수송에 중요한 역할을 한다. 이처럼 Rab 구아노신삼인산-가수분해효소의 다양한 역할을 수행할 뿐 아니라 Rab 경로의 교란은 많은 질병을 야기하기 때문에 Rab 구아노신삼인산-가수분해효소에 대한 연구는 활발히 진행되고 있다. 한편, Rab 구아노신삼인산-가수분해효소의 생화학적 연구 및 Rab 관련 기능연구에서 Rab 의 변이형 유전의 사용은 예전부터 중요하게 여겨왔었다. Rab 의 변이형 유전자를 구축할 때, 기존에 성공적으로 만들어진 다른 변이형 Rab 의 변이위치를 참조하는 방식을 일반적으로 사용했었다. 하지만 구조가 비슷한 Rab 사이에서도 리간드 친화도나 효소활성 및 상호작용하는 파트너 단백질의 종류가 서로 다르듯이, 비슷한 부위의 아미노산을 변이시켜 만든 효소 또한 서로 다른 활성형태를 가질 수 있다. 이러한 관점에서 새로운 변이형 유전자를 구축하게 되면 매번 생화학적, 구조적

측정을 통해 기능과 및 메커니즘이 어떤 양상을 보이는지 반드시 확인하여야 한다. 이러한 이유로 나는 Rab 구아노신삼인산-가수분해효소의 변이형 유전자가 가지는 특성들에 대해 연구하기 시작했다. 나는 본 연구에서 Rab6A'과 Rab11A 의 변이형 유전자를 결결정화하는데 성공하였고, 그들의 결정구조를 규명하였다.

나는 이 논문의 첫 파트에서 Rab6A'의 활성형 변이 유전자의 결정구조를 규명하였고 이 변이형 유전자가 구아노신이인산을 가질 수 있다는 것을 발견하였다. 이는 효소에 따라 리간드 결합이 다양하게 일어날 수 있으며, 효소 주위의 환경에 영향을 받을 수 있음을 시사한다. 본 논문의 두번째 파트에서는 Rab11A 의 비활성형 변이 유전자의 안정성은 구아노신이인산에 의해 결정될 수 있음을 발견하였다. 끝으로 마지막 파트에서는 Rab11A 의 활성형 변이 유전자가 GTP 를 분해하지 않은 상태로 결합하고 있는지를 구조적인 관점에서 해석하였다. 나의 연구는 Rab6A 와 Rab11A 가 Rab 네트워크와 질병에서 기능적 상호관계가 있음을 구조적인 관점에서 해석할 수 있는 단서를 제공하였다.

주요어 : 저분자량 구아노신삼인산 결합단백질, Ras 대가족 단백질, Rab 구아노신삼인산 가수분해효소, Rab6A, Rab11A, 세포막 수송, 단백질 결정구조

학 번 : 2009-21890